TECHNICAL MEMORANDUM

84

Evaluation of the gridpoint model and the new spectral model for the period 2 April to 20 April 1983

O. Åkesson, H. Böttger and R. Nieminen

Research Department

November 1983

European Centre for Medium-Range Weather Forecasts
Europäisches Zentrum für mittelfristige Wettervorhersage
Centre européen pour les prévisions météorologiques à moyen

ABSTRACT

For the period of parallel forecasting 2 April to 20 April 1983, the ECMWF gridpoint model and the spectral model with the new envelope orography are compared. The objective verification of upper air forecasts reveals that the spectral model gives better results in almost all respects. In the lower and middle troposphere, the skill in the forecast has improved up to 24 hours in the later stage of the forecast and about 12 hours around day 4 and 5, both at 1000 and 500mb in the Northern Hemisphere. The introduction of the envelope orography has a large impact on the surface fields and introduces strong biases, especially in the surface temperature and precipitation forecast in areas which are mostly affected by the change in the orography.

1. Introduction

The new spectral model and the new orography were introduced operationally on 21 April 1983. Prior to this, the new model was tested quasi operationally during the period 2 April to 20 April 1983 when parallel analyses and forecasts were produced from the spectral and the gridpoint models. For this period the two forecasting systems can therefore be compared with each other in an unbiased way as identical initial data sets were available to both systems. There were some problems in the first half of the period when e.g. many PAOBs were erroneously missed in the spectral assimilation. However, these differences are expected to have only little impact on the results.

The purpose of this paper is to present the results of these comparisons for internal use at ECMWF. It is assumed that the reader has some knowledge of the new forecasting system and the new orography. A revised version of the ECMWF Forecast Model Documentation manual is currently in preparation.

2. The data

During the time of the parallel forecasts the operational gridpoint model was postprocessed in the normal way. Special arrangements were made to postprocess the output from the test forecasts of the spectral model under quasi-operational conditions. The number of forecast steps for which the postprocessing was carried out was reduced to ten, every 24 hours at forecast time 24, 48, 72,...., 216, 240. Otherwise the upper air and surface data used in this comparison were available in the same format and on the same grid from both models.

The objective verification of upper air fields is carried out using the verification data base which includes gridpoint fields on a 3 by 3 degree resolution for the eight pressure levels 1000, 850, 700, 500, 300, 200, 100, and 50 mb for the parameters temperature, height and the u and v wind component. The verification of surface parameters (such as temperature at 2 metres, windspeed at 10 metres and precipitation amount against observations) from selected sites in Europe was carried out using data from the European archive which contains the surface fields on a 1.5 by 1.5 degree grid. The surface fields from the spectral model were originally available on the model's Gaussian grid, but were then interpolated to the same standard grid of the European

archive by means of the routines which are now used operationally to convert the data. The interpolation of forecast values to the location of the observing site is done linearly from the four surrounding gridpoints.

Forecasts from the spectral model were completed to 10 days in 16 cases, but on three days during the period of the parallel forecasts the test forecast of the spectral model was abandoned for operational reasons before reaching the last forecast step. When comparing the two forecasting systems objectively, only those forecasts available from both the spectral and the gridpoint model were included.

3. The synoptic situation in April 1983

In the Northern Hemisphere a high index circulation type was established for much of the month. In a lively westerly flow, pronounced but mobile troughs moved across the North Pacific, over North America, and across the North Atlantic into Europe. No indication of a developing blocking trough-ridge system was observed, though the long waves amplified considerably towards the end of the period of this comparison.

Over the Southern Hemisphere quite an amplified long wave activity was observed over southern Australia and the adjacent sea areas at the beginning of the month. Deep troughs also occurred both on the windward and on the lee side of the Andes. The amplitudes of the long waves decreased towards the middle of the month, exhibiting some tendency to increase again thereafter. A cut-off low was observed at 500 mb over Tasmania, south of Australia, after 15 April.

In general the predictability was quite low during the month of April. Compared to April 1982 the skill of the operational forecast was reduced by almost 12 hours in the lower and middle troposphere over the Northern Hemisphere when using the 60% value of the anomaly correlation of height as a limit of predictability. In the Southern Hemisphere, however, the performance of the model had slightly improved compared to April of the previous year. This should be borne in mind when comparing the objective scores from the two forecast systems.

4. Results

4.1 Objective verification of upper air fields

Identical data sets from both forecast runs were used in this verification. The operational forecasts were omitted from days on which the spectral forecast was

missing. The forecasts have been verified against the initialised analyses using the operational analysis for the gridpoint model and the test analysis for the spectral model.

A modified version of the operational field verification system was used. The areas for North America and China-Japan were displaced to the east and similarly the area over India was moved southwards to avoid the highest mountains, as shown in Fig. 1. The height and temperature forecasts were verified at 8 levels over the hemispheres and the tropical belt and in three limited areas: Europe, North America and China-Japan in the Northern Hemisphere and over the Australian-New Zealand region in the Southern Hemisphere. The wind forecasts were verified only at the 850 and 200 mb levels over the tropical belt and the limited areas of India and Indonesia.

Figs. 2 to 15 show the pressure time sections for the anomaly correlation, standard deviation of error and mean error of height and temperature forecasts for the operational gridpoint and the experimental spectral model. The mean values of the anomaly correlation and the standard deviation of the 1000 and 500 mb height forecasts are presented in Figs. 16 to 18. Similarly the mean values for the absolute correlation and the rms-error of the vector wind at 850 and 200 mb in the tropics are shown in Figs. 19 and 20. Finally, the systematic error of height at 1000 and 500 mb and of temperature at 850 and 500 mb for the hemispheres and the tropical belt is given in Figs. 21 and 22.

For both the anomaly correlations and the standard deviation of height and temperature the spectral model gives generally better results in the Northern Hemisphere. This can be seen from both the hemispheric and the limited area scores. The improvement in the Northern Hemisphere forecasts is about 12 hours in the 4 to 5 day forecasts and in the order of 24 hours in the 7 to 9 day forecasts at both 1000 and 500 mb (Fig. 18). For the Southern Hemisphere the differences in the verification results between the two models are smaller, but they still indicate an overall improvement in the lower troposphere for the height forecasts. In the limited area of Australia and New Zealand the operational gridpoint model has some advantage over the spectral model.

The results from the wind verification in the tropics (Figs. 19 and 20) show very small differences between the two models. The spectral model gives slightly smaller vector wind errors at the 200 mb level than the gridpoint model.

The mean error of height (Fig. 21) and temperature (Fig. 22) reveals a feature common to all verification areas. The negative bias in the area mean values has increased in the spectral model. For the temperature forecasts the cooling effect is most pronounced at the lower tropospheric levels. It decreases with height and positive temperature biases are observed around the tropopause. The mean height error is found to reach its maximum in the middle of the troposphere and some compensation due to the different vertical structure of the temperature error occurs at higher levels of the troposphere. These effects which imply different values for the hydrostatic stability of the model atmosphere compared with that of the old gridpoint model are most pronounced in the tropics. Changes in the radiation parameterisation introduced operationally early in May compensated the cooling but hardly reduced the positive bias near the tropopause (see para. 6).

The negative bias in temperature appears to be smaller in the Northern Hemisphere than in the Southern Hemisphere and the tropics. The mean error charts (see chapter 4.2) show that the largest negative values are found over the oceans.

4.2 Mean error fields of height

Hemispheric mean error charts of height for both the Northern Hemisphere and Southern Hemisphere are presented in Figs. 23-32. The global error distribution is more or less the same for the two models, with maxima over Europe, the Atlantic and the Pacific in the Northern Hemisphere. The Atlantic maximum grows the fastest and is by far the dominant error feature at +240 hours. For the Southern Hemisphere there is one persistent area of growing negative error between South America and the Antarctic which between day 5 and day 7 of the forecast merges with another negative error area moving westwards from the South Pacific. After 120 hours an area of developing negative error is found south of New Zealand which reaches its maximum around 168 hours of forecast time in both models.

Areas where the test forecasts produces smaller absolute errors than the operational forecasts include much of northern Asia (at 500 mb only), northern Europe and the Atlantic in the medium range, the eastern Pacific from the Rockies to 180 W, the area around 65 S, 0 E in the South Atlantic and the area to the south and south-east of Africa from day 7 onwards.

Areas where the operational model performs better include the western Pacific, the eastern part of Asia, the area south of New Zealand (out to day 7) and the area between South America and the Antarctic (out to day 7).

The quasi-stationary error in both forecasts between the southern tip of Chile and the Antarctic is smaller out to day 7 in the operational forecasts. This pattern may be ascribed to the lack of realistic representation of the narrow but high mountain ranges of 2000-4000 m on both sides of the sound. In fact, on the Antarctic side, the new model has even lower mountains (about 200m) than the operational model (about 1000m) due to the iterative correction procedure. In mountainous regions except for the Himalayas, there are on average smaller errors in the test set, particularly at 1000 mb.

4.3 Verification of surface parameters

The verification of surface weather parameters was carried out at eight locations in Europe for temperature at 2 metres and wind speed at 10 metres above the model surface and for precipitation amounts accumulated over 24 hours. The stations are listed in Table 1 and their location is shown in Fig. 33. Nearly all the stations are affected by changes in the model's orography or changes of the coastlines. For comparison Hannover and the ocean weather ship (OWS) Lima were included as locations, where only minor effects on the surface parameters by the model changes were expected to be seen. All the model predictions were compared to observations taken at 12 GMT. The stations chosen are notable for their reporting reliability. Even so, complete records for all stations for this time period were not available. Care was taken that only events which were available for both forecasts went into the comparison. The 48 hour and the 72 hour forecasts were verified at the eight locations. As the sample is fairly small the result can only be described in general terms. Time graphs (meteograms) are shown to highlight typical differences between the two forecasts rather than objective verification scores. The change in the model orography had an expected impact on the mean error of temperature forecasts while any other systematic differences of local wind and precipitation forecasts between the two models are more difficult to establish from the short period of this comparison.

Figs. 34 and 35 show the predicted temperature at 2 metres, windspeed at 10 metre and precipitation amount (accumulated over the previous 24 hours) valid at 12 z on day 2 of the forecast compared to the observations at Limoges in France. Figs. 36 and 37 show meteograms only for forecasts valid on day 3.

The temperature forecasts are very similar from both the gridpoint and the spectral model. The negative bias has increased due to the higher elevation of the new orography at this station. This change in the mean error of course varies from station to station depending on the details of the orography changes (see Table 2). For stations such as Hannover, Stockholm or

WMO Index No.	Name	Latitude	Longitude	Height	Model Height
10866	Munich	48.13N	11.72E	529 m	1760 m
11036	Wien	48.12N	16.57E	190 m	865 m
16420	Messina	38.20N	15.55E	51 m	2 m
02464	Stockholm	59.35N	17.95E	11 m	78 m
17600	Cyprus	34.75N	32.40E	9 m	- 109 m
10338	Hannover	52.47N	9.70E	54 m	13 m
07434	Limoges	45.87N	1.18E	402 m	498 m
	OWS Lima	57.00N	20.00W		- 23 m

Table 1: List of stations used in local verification of surface parameters.

	Spectral model	Gridpoint model	Δ	Spectral model	Gridpoint model	Δ
Stockholm	-3.20	-3.34	.14	-4.20	-3.71	-.49
Wien	-6.17	-3.24	-2.93	-7.50	-4.53	-2.97
Hannover	-2.19	-1.95	-0.24	-2.67	-3.39	.72
Messina	-3.06	-4.08	1.02	-3.83	-4.05	.22
Munich	-10.99	-4.48	-6.5	-12.13	-5.59	-6.54
Limoges	-4.04	-1.85	-2.19	-4.01	-1.80	-2.21
Cyprus	-2.58	-2.70	.12	-3.58	-2.97	-0.61
OWS Lima	-0.69	.17	-0.86	-0.33	.81	-1.14

Table 2: Comparison of mean error of temperature (2m) forecasts from spectral and gridpoint model at eight locations in Europe, period 2-20 April 1983.

Cyprus where the changes of the model orography had only little effect on their new station height in the model, the change in the bias is negligible and may be ascribed to the variability inherent in small data samples. The negative change in the mean error at OWS Lima seems to be significant. It increases with forecast time and is in agreement with an increasing cooling in the lower troposphere shown in 4.1 especially over sea areas. With only one exception the standard deviation (not shown) of the predicted temperature for all the eight stations has increased slightly giving a desirable increase of the predicted temperature range.

While the temperature forecasts from both models were very similar, larger differences occurred in the forecast of the windspeed and were even more pronounced in the precipitation amounts. It is not possible to arrive at a conclusion as to which of the two forecasts is to be preferred as the verification sample is too small. The predicted precipitation amount is very much influenced by minor forecast errors which may explain the differences between the two forecasts when verifying them locally against observations. No systematic defects or biases could be detected in the precipitation forecasts of the new spectral model in these local verifications.

The predicted 10 metre wind on the other hand exhibits a tendency towards increasing the negative bias observed in previous verifications of the gridpoint model. This can be seen most clearly in the results for Cyprus. Fig. 38 shows the 72 hour forecast of the 10 metre wind speed for the two forecast models. There is clearly a better fit to the observations by forecasts taken from the operational gridpoint model. For the other locations in Europe the differences are much smaller. Cyprus is an island in the eastern Mediterranean and sheltered by high mountains over Turkey and Lebanon. These mountains have been raised in the new orography. The negative bias in the windspeed over the eastern Mediterranean may partly be attributed to this change. The results for OWS Lima exhibit no systematic change in the forecast of windspeed over the oceans. Figs. 39 and 40 give the verification of the 72 hour forecasts of temperature, windspeed and precipitation amount at the location of the ocean weather ship in the North Atlantic. No systematic difference between the two forecasts can be detected for any of the three parameters.

4.4 Synoptic assessment based on case studies

The day to day differences between the results from the two models are in most cases minor, especially in the early stages of the forecasts, but on a few occasions some significant differences developed between the spectral and the operational gridpoint model output. In the following some examples are given.

4.4.1 Height field

At times, during the period of the parallel forecasts, weak troughs or lows developed south of the Alps. Fig. 41 shows one of these situations with an analysed 1000 mb low over Poland and a trough extending to the northern Mediterranean. The spectral day 5 forecast in Fig. 41 gives an overdeveloped low over northern Italy while the gridpoint model does not capture the intensity and displaces the trough eastward. The Polish low is incorrectly positioned in both forecasts and appears to be weaker in the spectral forecast. The overdevelopment of lows in the lee of the Alps was also found in previous evaluations of envelope orography experiments, and may be regarded as a systematic error.

The two day 8 surface forecasts valid on 11 April give a completely different picture of the flow pattern over Europe (Fig. 42). Although both forecasts are misleading with strong phase errors particularly in the spectral forecast, the general appearance of the latter is more realistic compared to the gridpoint model forecast which shows an elongated low extending from southern Greenland across southern Scandinavia into western Russia.

A good improvement of the predicted 500 mb low pattern over Europe in a day 6 forecast of the spectral model is shown in Fig. 43. The gridpoint model shows the "typical" systematic error which occurs in situations when a cut-off low develops in the Mediterranean.

4.4.2 Precipitation amount

On the forecasts from 11 to 13 April respectively verifying on 14 April, there are large differences in the the total amounts of precipitation accumulated over 24 hours between the spectral (Fig. 44) and the gridpoint model forecasts (Fig. 45). Note that there is a 12 hour lag (associated with the postprocessing of the spectral model during the time of the parallel forecasts) between the forecasts shown in the two figures, and this may explain some of the differences. The amounts from the operational model are for the period 00Z to 24Z valid on the forecast day, while the test forecast was only postprocessed every 24 hours at 12z and the precipitation amounts therefore accumulated over the 24 hours from the previous forecast day up to 12z of the indicated valid time. However, the difference is in the order of factor 2 to 3 for the maximum amounts predicted over central and eastern parts of North America. Systematically larger amounts are predicted by the operational model. Some observed values corresponding to the accumulation time of the test and the

operational forecast are shown for this area in Fig. 46. The observations show the maximum amounts of the same order as those predicted by the gridpoint model. In both forecasts the precipitation is spread out over too large an area; this is especially notable for the spectral forecast.

In the region west of Portugal and in the precipitation band oriented in a north-south direction over the Atlantic the spectral model gives smaller amounts than the gridpoint model. Over Europe the differences are small and randomly distributed between the two models. Large differences, however, can be seen in the day 3 forecast of 13 April (Fig. 47). Over southern and eastern Europe the gridpoint model again predicts larger amounts.

The precipitation amounts seem to be increased in the tropics for the spectral model. In an arid area such as Yemen much higher amounts of convective rain is predicted up to day 3 for 14 April (Fig. 48). Also other areas such as southern parts of the Himalayas and Bangladesh or Madagascar are found to receive more rain by the spectral forecast compared to the gridpoint model prediction, at least for this forecast.

4.4.3 Surface parameters

The cooling especially near the surface which has been mentioned earlier on in this report is illustrated by three meteograms from 14 April including graphs of various surface parameters. They are valid for stations in North Yemen, central Borneo and central Africa. Fig. 49 and 50 show the meteograms for the spectral model and the operational model respectively. The cooling trend in the spectral forecast is shown by the surface and the 2 metre temperature and dewpoint in the uppermost graphs.

The second graph from the top shows the precipitation amounts. There are large differences only for North Yemen. This is in agreement with the precipitation fields shown in Fig. 48. In accordance with the difference in the predicted rain amounts the soil wetness increases in the test forecast but remains at zero in the operational model. Graph 4 shows the latent and the sensible heat fluxes. The differences are small for the latent heat fluxes. The sensible heat flux, however, is positive with values of 30 to 50 watts/m**2 in the test forecast for Borneo and central Africa while it stays around zero in the operational model prediction for these points.

5. Recent changes to the operational forecasting model

Early in May 1983 a modification was introduced to the operational forecasting model changing the parameterisation of aerosols in the atmosphere. This

modification corrected the excessive cooling which was observed in the lower model troposphere after the introduction of the spectral model (see para. 4.1). The impact of the change can clearly be seen in the daily average temperature errors at 1000 and 850 mb from 15 April to 15 May 1983 (Fig. 51). However, the positive temperature bias near the tropopause in the tropics remained.

6. Summary

We have evaluated the forecasts from the gridpoint model and the new operational spectral model for the time of the parallel forecast period 2 to 20 April 1983. In addition to the objective field verification for the Northern and Southern Hemispheres and the tropics and some limited areas we have looked at the verification of surface parameters at some locations in Europe and have attempted a synoptic evaluation based on some case studies. The new spectral model gives better results in almost all respects. It is clearly superior when assessing the objective scores. The improvement in the forecast can best be seen in the objective scores for the height fields. In the lower and middle troposphere the skill in the forecast has improved up to 24 hours in the later stage of the forecast and about 12 hours around day 4 and day 5 both at 1000 and 500 mb in the Northern Hemisphere for the period of these parallel forecasting experiments. The improvement varies slightly for the limited areas and is less obvious for the Southern Hemisphere, where data problems in the spectral assimilation might have had some influence. Objective scores for the local verifications of surface weather parameters and synoptic case studies of the flow and some surface fields have to be treated with caution as the sample is small. The parameter affected most by the change in the orography is the temperature close to the model surface. Height differences between the altitude of an observing site and the height of the model surface at the same location will introduce a bias in the surface temperature. This can partly be reduced by applying a temperature correction based on a moist adiabatic vertical gradient.

List of Figures

Objective verification of upper air field

Mean error fields of height

Fig. 23 Mean height error for the ensemble of 24 hour forecasts for the Northern Hemisphere
Upper left: 500mb spectral forecast
Upper right: 1000mb spectral forecast
Lower left: 500mb grid-point forecast
Lower right: 1000mb grid-point forecast
Units in m, contour interval: 10m

Fig. 24 Same as Fig. 23 but for 72 hour forecasts
Contour interval: 40m for 500mb forecasts, 20m for 1000mb forecasts

Fig. 25 Same as Fig. 24 but for 120 hour forecasts

Fig. 26 Same as Fig. 24 but for 168 hour forecasts

Fig. 27 Same as Fig. 24 but for 240 hour forecasts

Fig. 28 Same as Fig. 23 but for the Southern Hemisphere

Fig. 29 Same as Fig. 24 but for the Southern Hemisphere

Fig. 30 Same as Fig. 25 but for the Southern Hemisphere

Fig. 31 Same as Fig. 26 but for the Southern Hemisphere

Fig. 32 Same as Fig. 27 but for the Southern Hemisphere

Verification of surface parameters

Fig. 33 Locations of stations used in verification of surface weather parameters.

Fig. 34 Verification of near surface parameters at Limoges for temperature at 2m, windspeed at 10m and precipitation amount (from top to bottom). Full line is the observation, dashed line is the 48 hour forecast from the operational gridpoint model. Period 2-18 April 1983.

Fig. 35 Same as Fig. 34, dashed line gives the 48 hr forecast from the spectral model.

Fig. 36 Verification of near surface parameters at Limoges for temperature at 2m, windspeed at 10m and precipitation amount (from top to bottom). Full line is the observation, dashed line is the 72 hour forecast from the operational gridpoint model. Period 2-18 April 1983.

Fig. 37 Same as Fig. 36, dashed line gives the 72 hour forecast from the spectral model.

Fig. 38 Verification of 72 hour forecast of windspeed (10m) at Cyprus. Full line is the observation, dashed line the forecast, top panel gives the result from the gridpoint model and the bottom panel the verification for the spectral model forecast, period 2-18 April 1983.

Fig. 39 Verification of near surface parameters at OWS Lima for temperature at 2m, windspeed at 10m and precipitation amount (from top to bottom). Full line is the observation, dashed line is the 72 hour forecast from the operational gridpoint model. Period 2-18 April 1983.

Fig. 40 Same as Fig. 39, dashed lines give the 72 hour forecast from the spectral model.

Synoptic assessment

Fig. 41 1000mb height (solid) and 850mb temperature (dashed) fields

Fig. 42 1000mb height and 850mb temperature D+8 spectral forecast (top), D+8 grid-point forecast (middle), and analysis (bottom) all valid at 12 GMT 11 April 1983.

Fig. 43 500mb forecasts (top and bottom row) and analysis (middle row) of geopotential height, valid time 12 GMT 13 April 1983. The upper left frame shows the 144 hour spectral forecast from 7 April 1983, the upper right the corresponding grid-point forecast. The lower left frame shows the 168 hour spectral forecast from 6 April 1983, the lower right the corresponding grid-point forecast.

Fig. 44 Precipitation accumulated from the spectral model during the period 12 GMT 13 April - 12 GMT 14 April 1983. (Unit: mm).
Top: 24 hour forecast from 13 April 1983
Middle: 48 hour forecast from 12 April 1983
Bottom: 72 hour forecast from 11 April 1983

Fig. 45 Precipitation accumulated from the grid-point model during the period 00 GMT 14 April - 00 GMT 15 April 1983. (Unit: mm).
Top: 36 hour forecast from 13 April 1983
Middle: 60 hour forecast from 12 April 1983
Bottom: 84 hour forecast from 11 April 1983

Fig. 46 Observed precipitation accumulated over 24 hours
Left: for the time period 12 GMT 13 April - 12 GMT 14 April 1983 (corresponding to the spectral forecast in Fig. 37).
Right: for the time period 00 GMT - 24 GMT 14 April 1983 (corresponding to the grid-point forecast in Fig. 37). (Unit: mm).

Fig. 47 Forecast precipitation accumulated over 24 hours for the 72 hour spectral forecast from 16 April 1983 (top) and the 84 hour grid-point forecast from 16 April 1983 (bottom). (Unit: mm).

Fig. 48 72 hour accumulated precipiation in the spectral forecast from 14 April 1983 (top) and the grid-point forecast from 14 April 1983 (bottom). (Unit: log; 1=1.7mm, 2=6.4mm, 3=19.1mm, 4=53.6mm, 5=147.4mm)

Fig. 49 Surface parameter meteograms for North Yemen (left), Central Borneo (middle) and Central Africa (right) from the spectral forecast of 14 April 1983.

Fig. 50 Surface parameter meteograms for North Yemen (left), Central Borneo (middle) and Central Africa (right) from the grid-point forecast from 14 April 1983.

Recent changes to the forecasting model

Fig. 51 Mean error of temperature in degrees Celsius for 850 mb (top) and 1000 mb (bottom) over the Northern Hemisphere (left) and the tropic (right), for day 1, day 3 and day 7 of the forecast in the period 15 April to 15 May 1983.

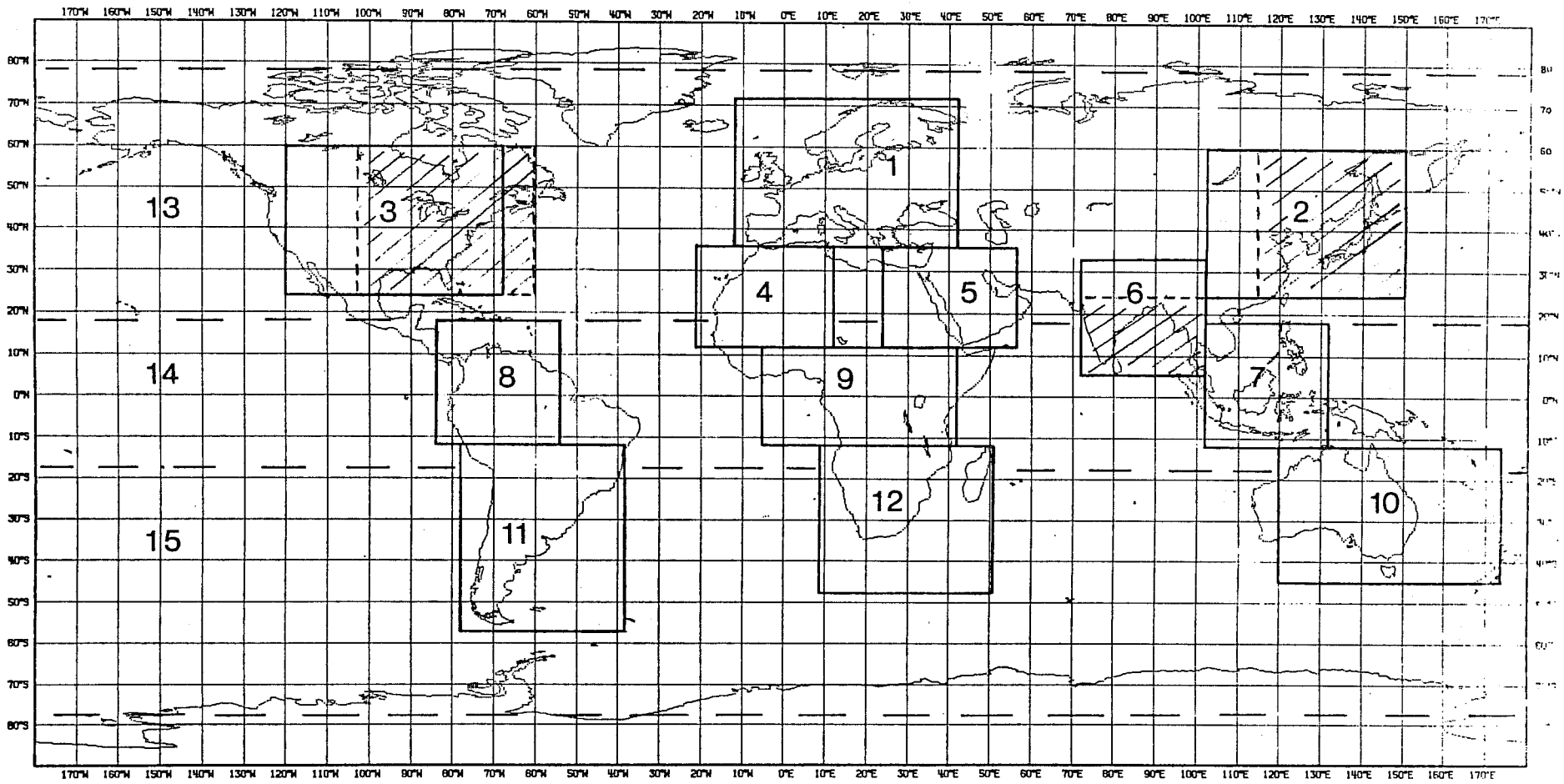

Fig. 1 The operational verification areas. (The hatching shows the modifications to areas 2, 3 and 6.)

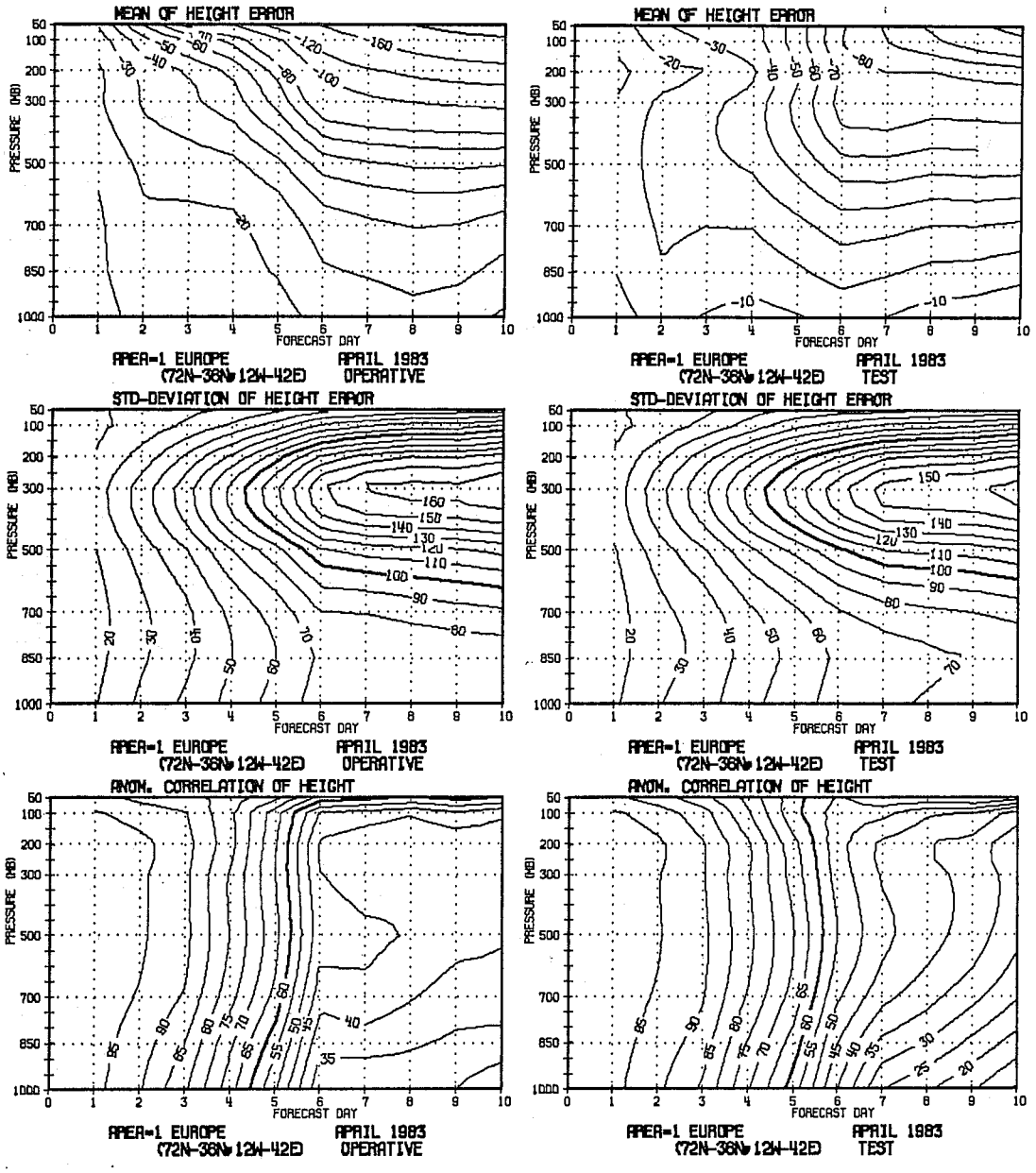

Fig. 2 Pressure-time section of mean error, standard deviation and anomaly correlation (top to bottom) for height over Europe. Verification of gridpoint model on the left and of spectral model on the right.

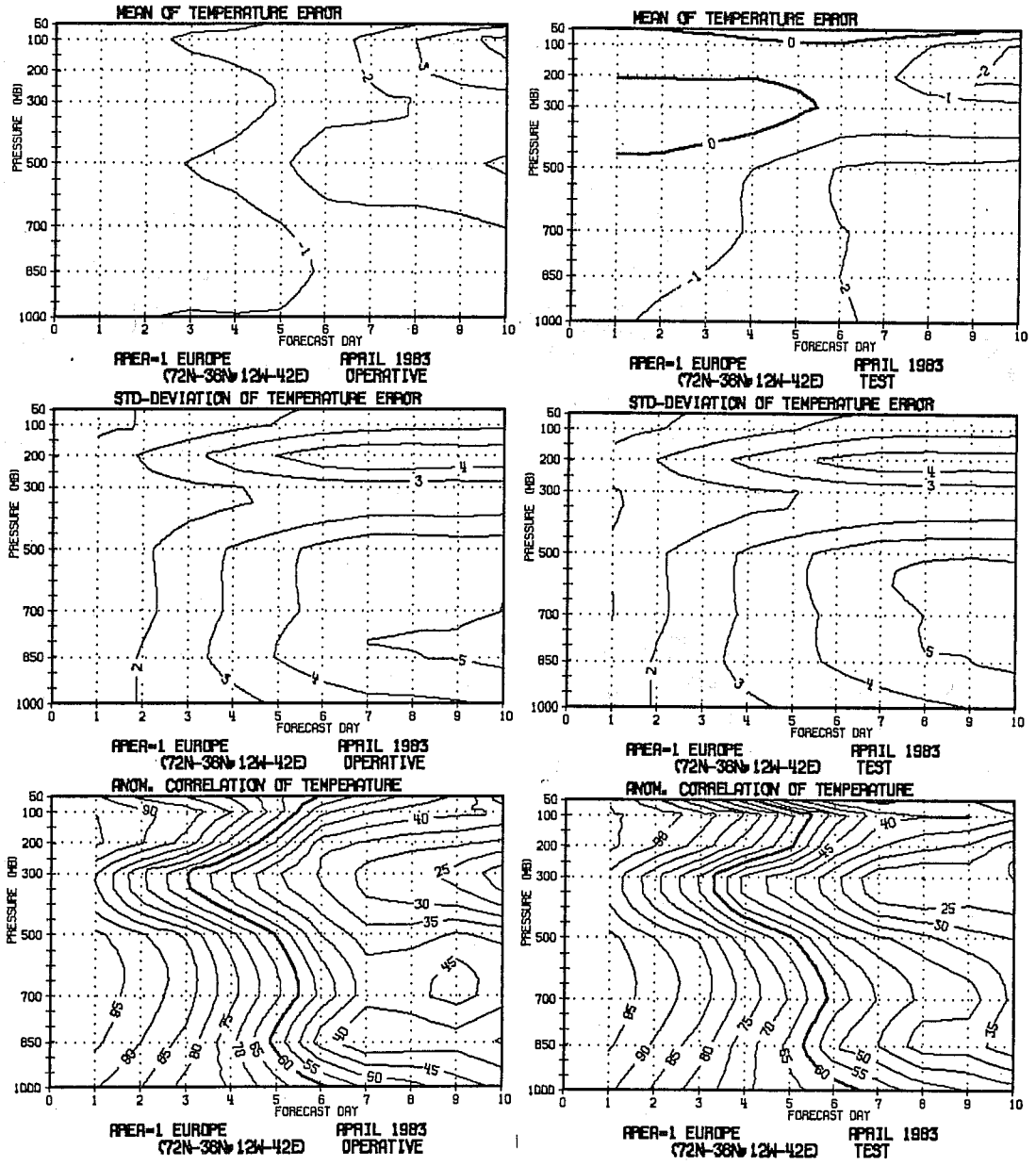

Fig. 3 As Fig. 2, for temperature.

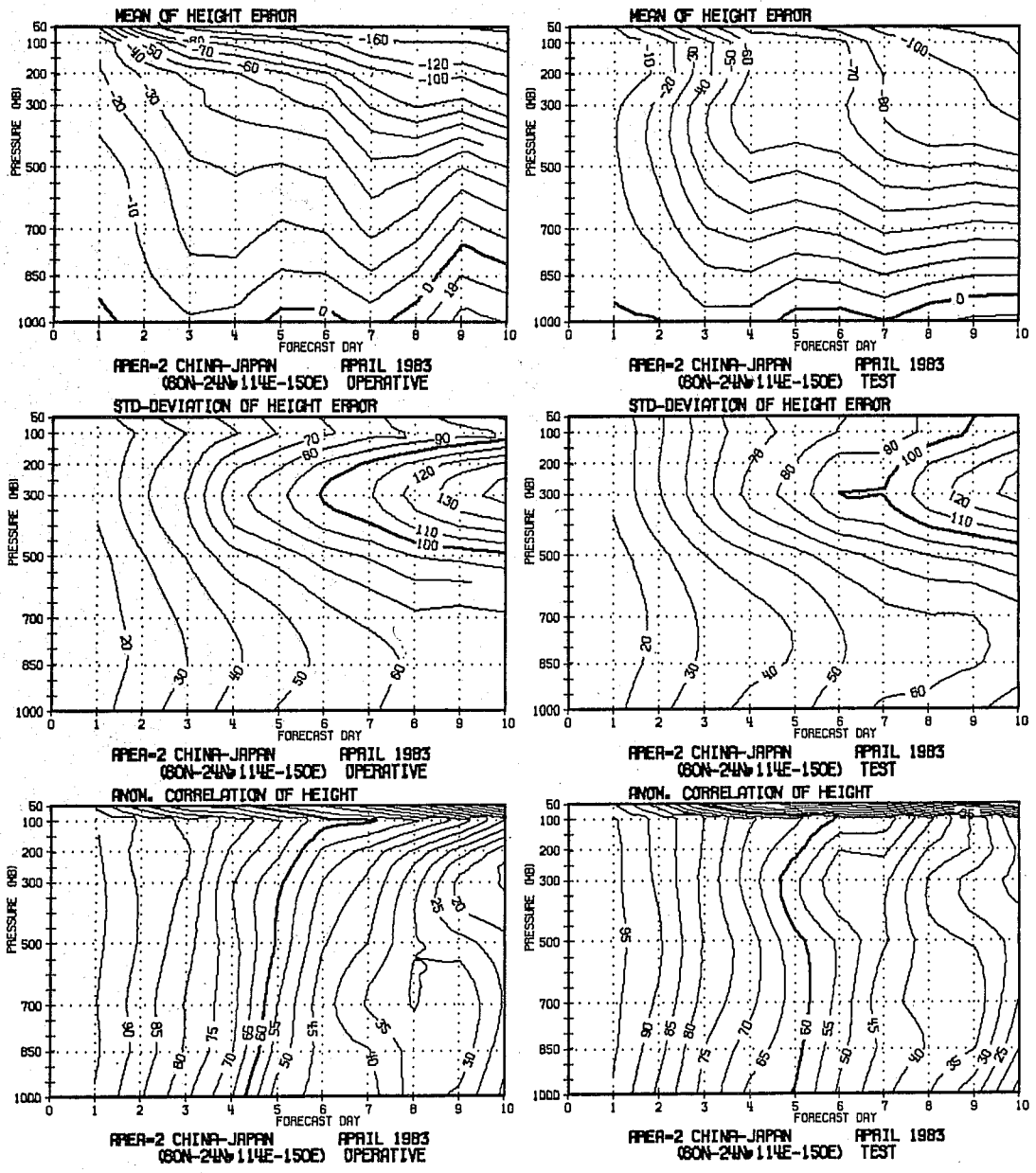

Fig. 4 As Fig. 2, for China - Japan.

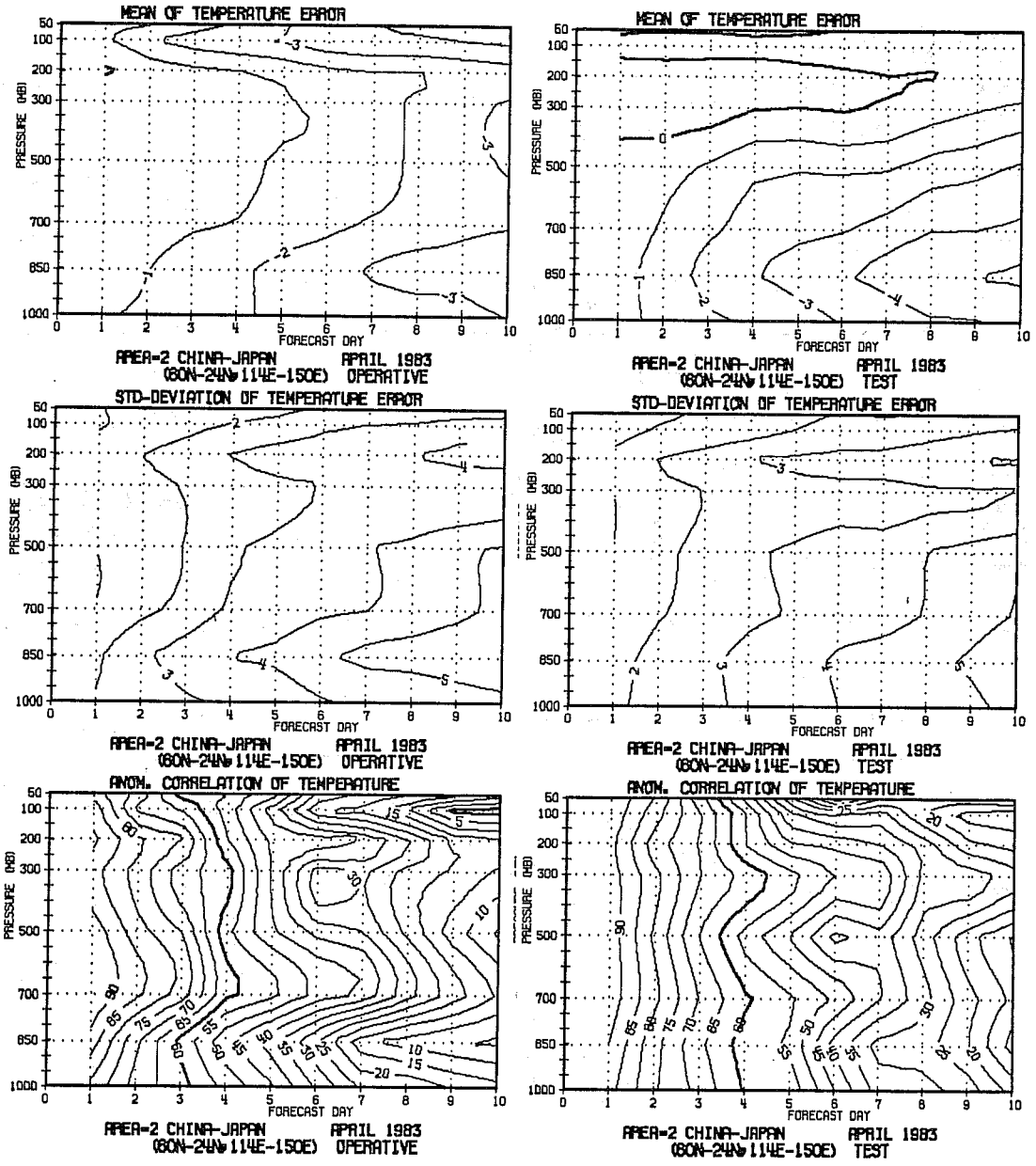

Fig. 5 As Fig. 2, for temperature over China - Japan.

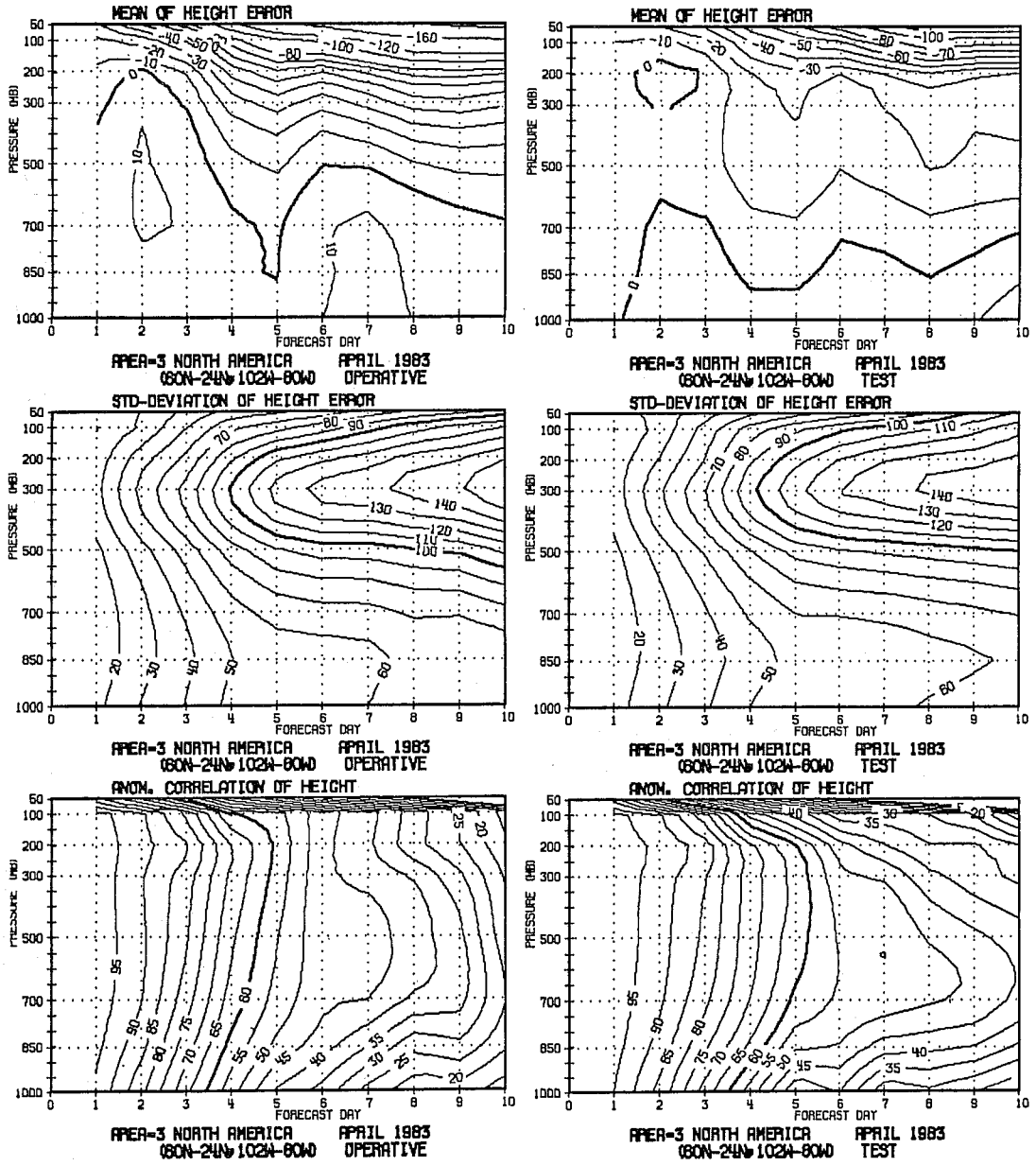

Fig. 6 As Fig. 2, for North America.

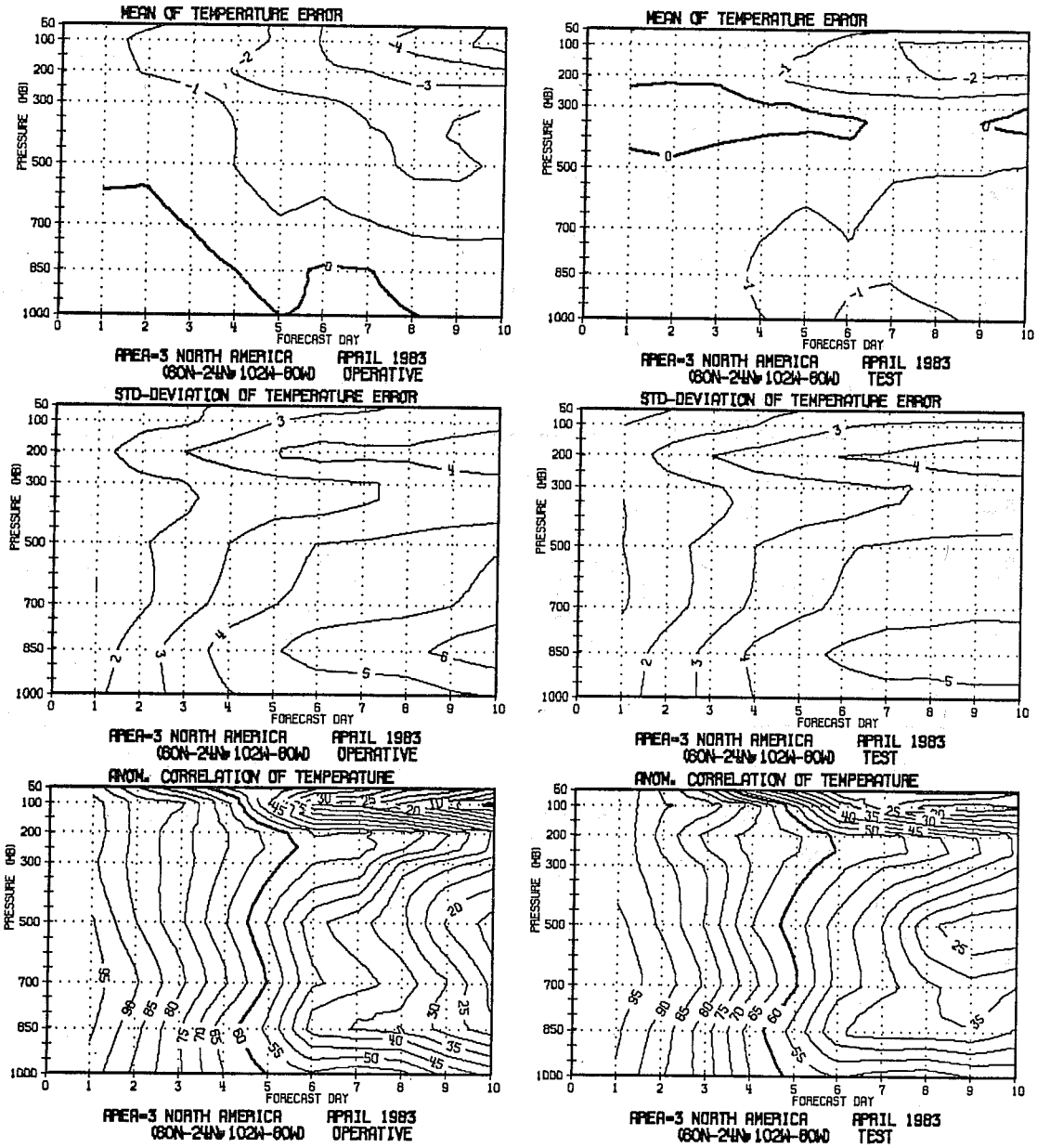

Fig. 7 As Fig. 2, for temperature over North America.

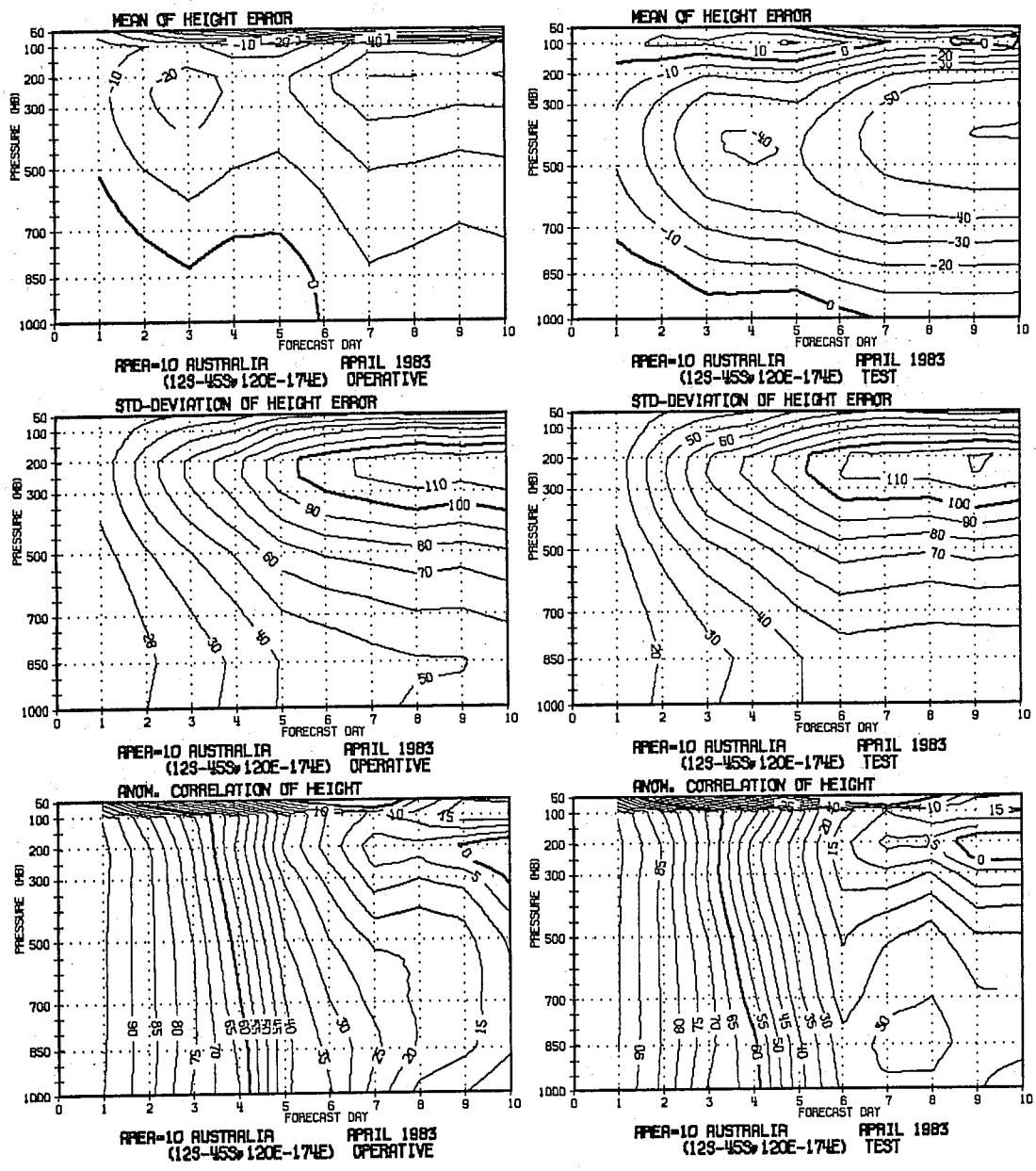

Fig. 8 As Fig. 2, for Australia.

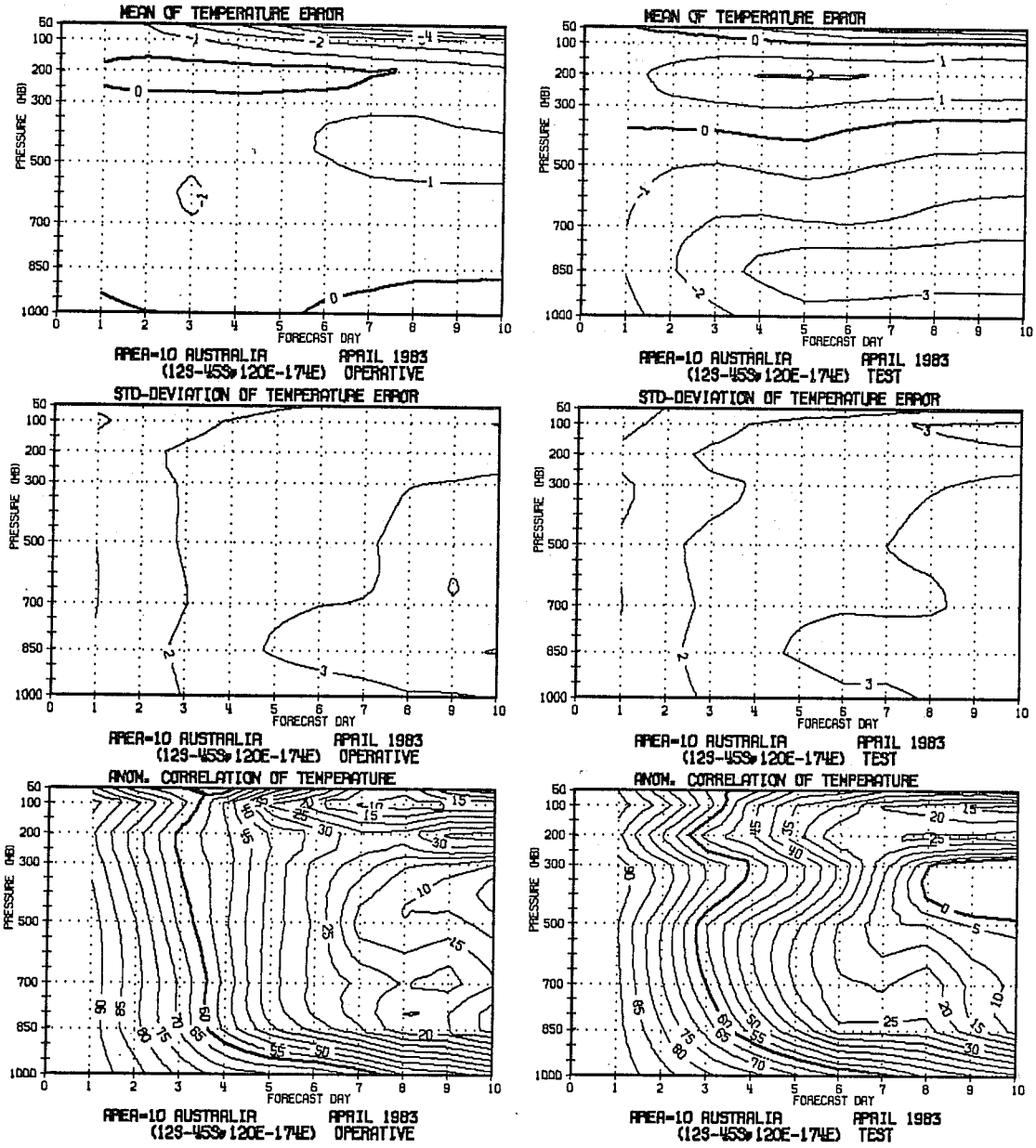

Fig. 9 As Fig. 2, for temperature over Australia.

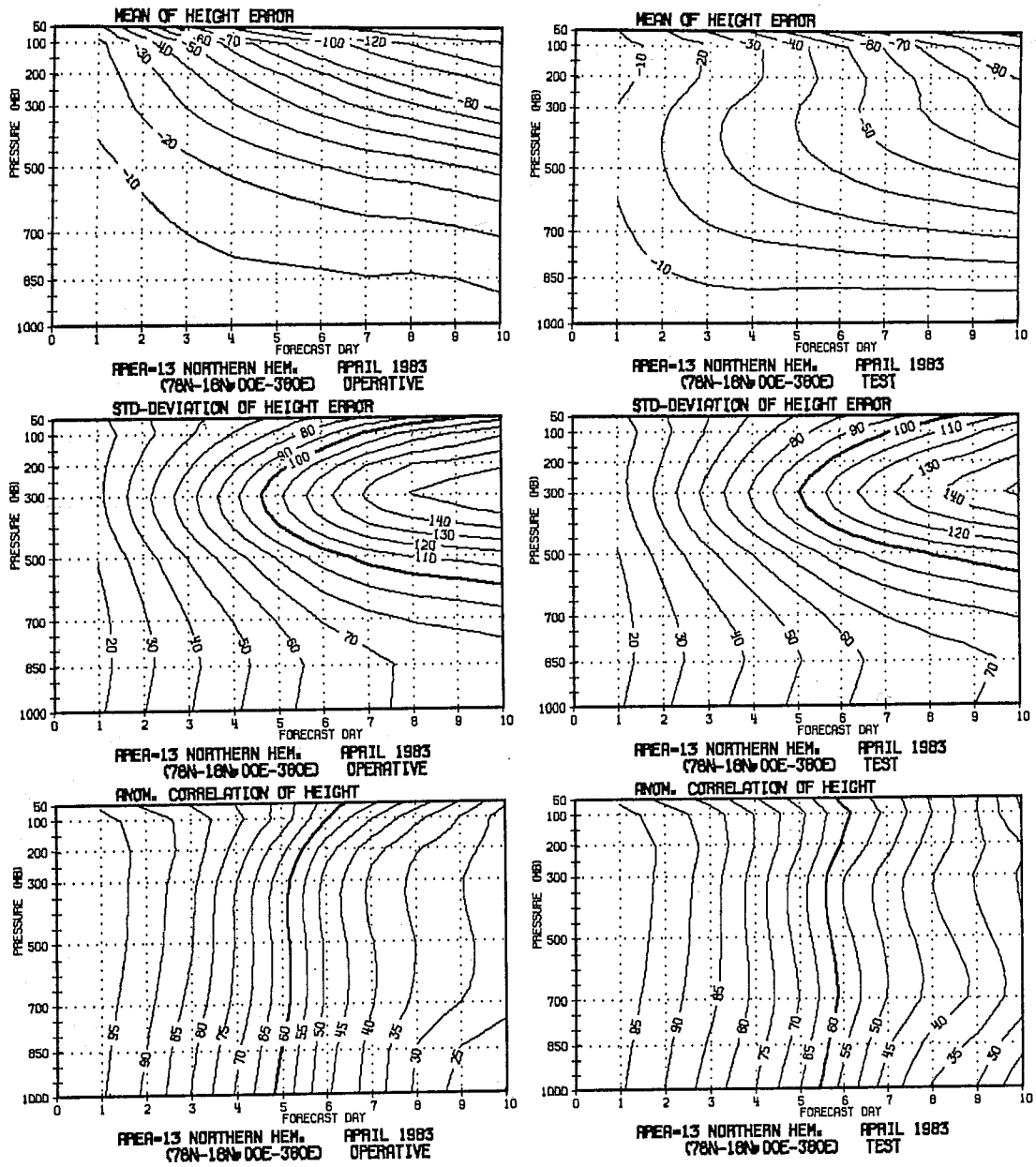

Fig. 10 As Fig. 2, for the Northern Hemisphere.

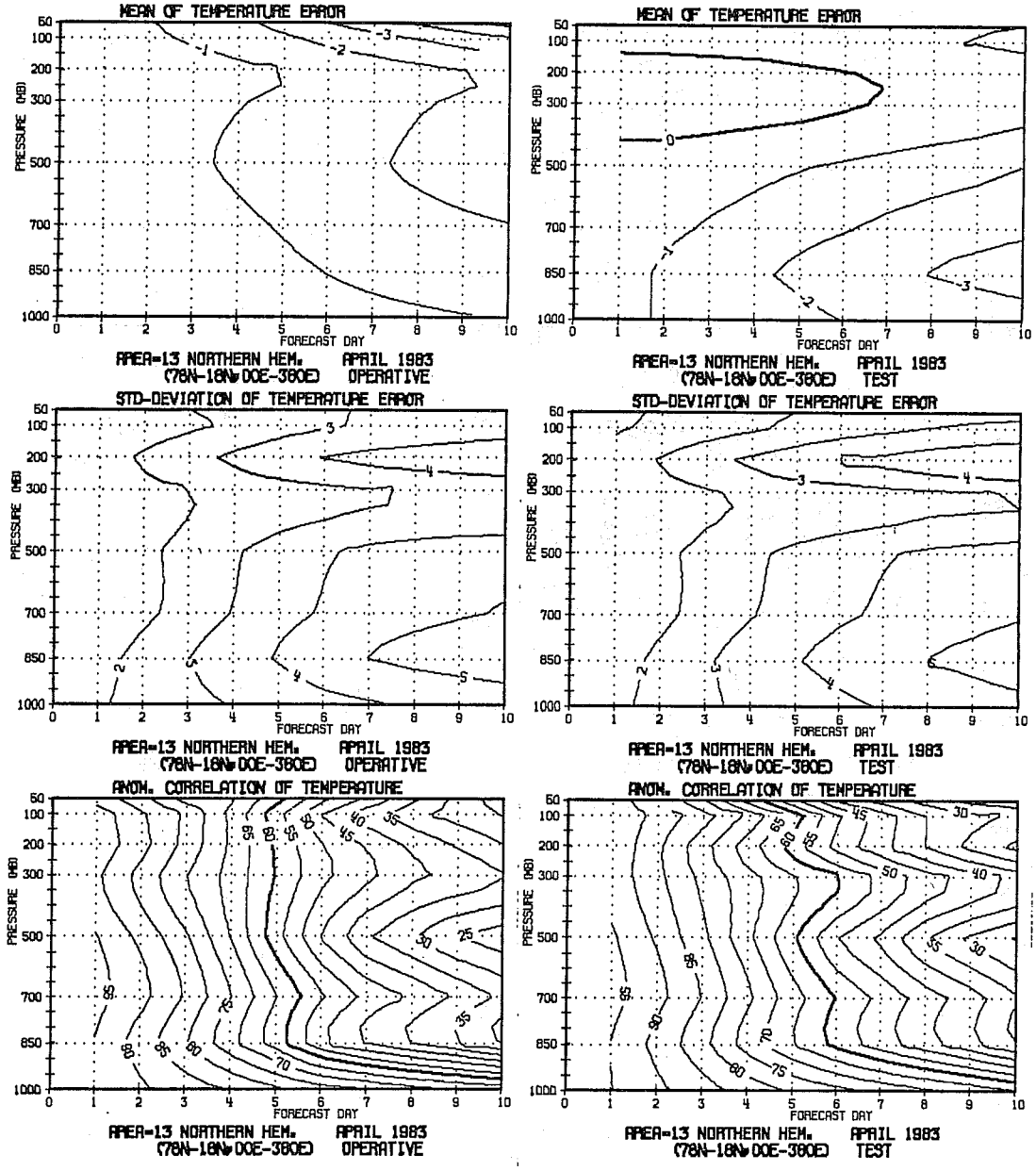

Fig. 11 As Fig. 2, for temperature over the Northern Hemisphere.

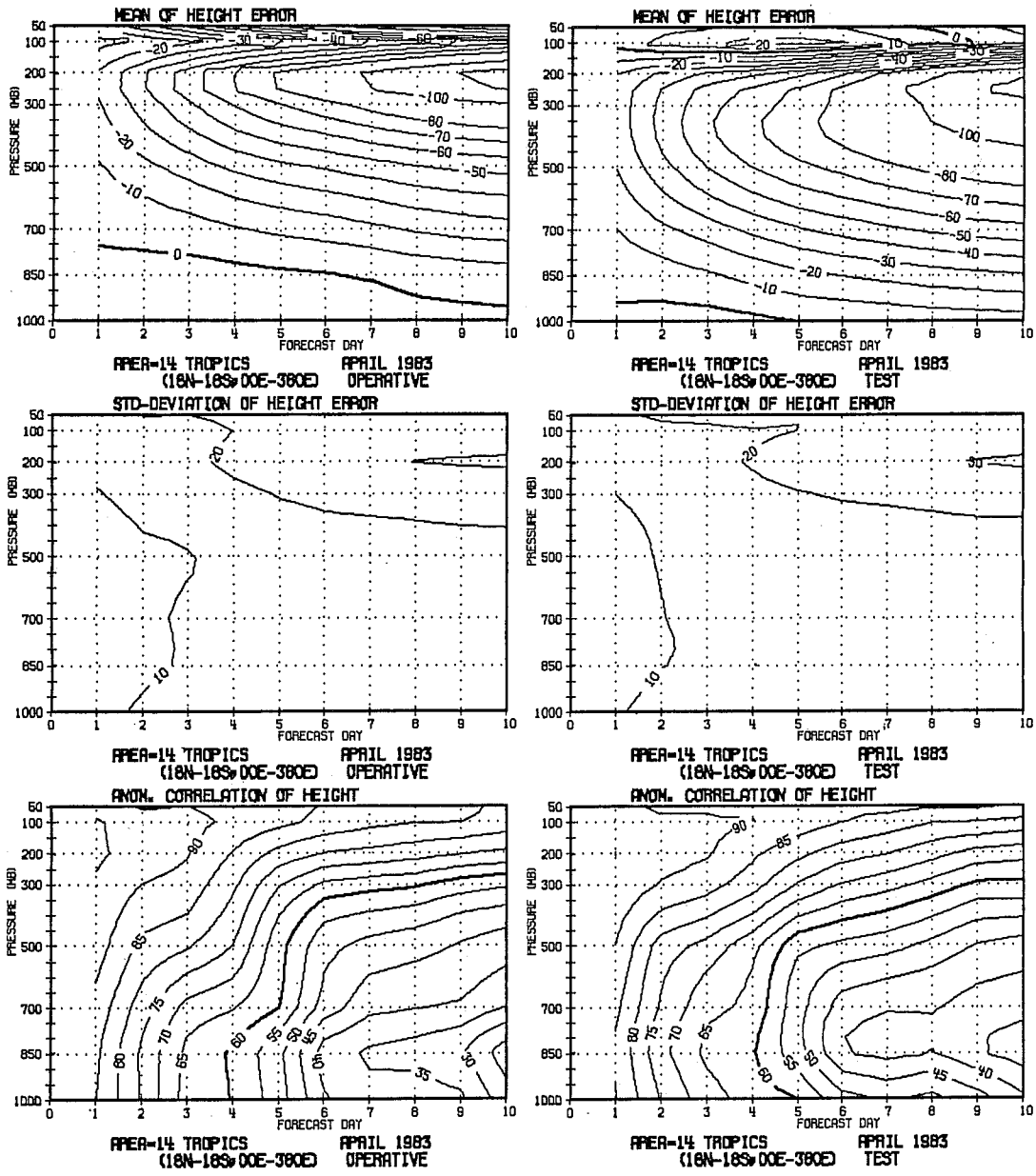

Fig. 12 As Fig. 2, for the tropical belt 18N to 18S.

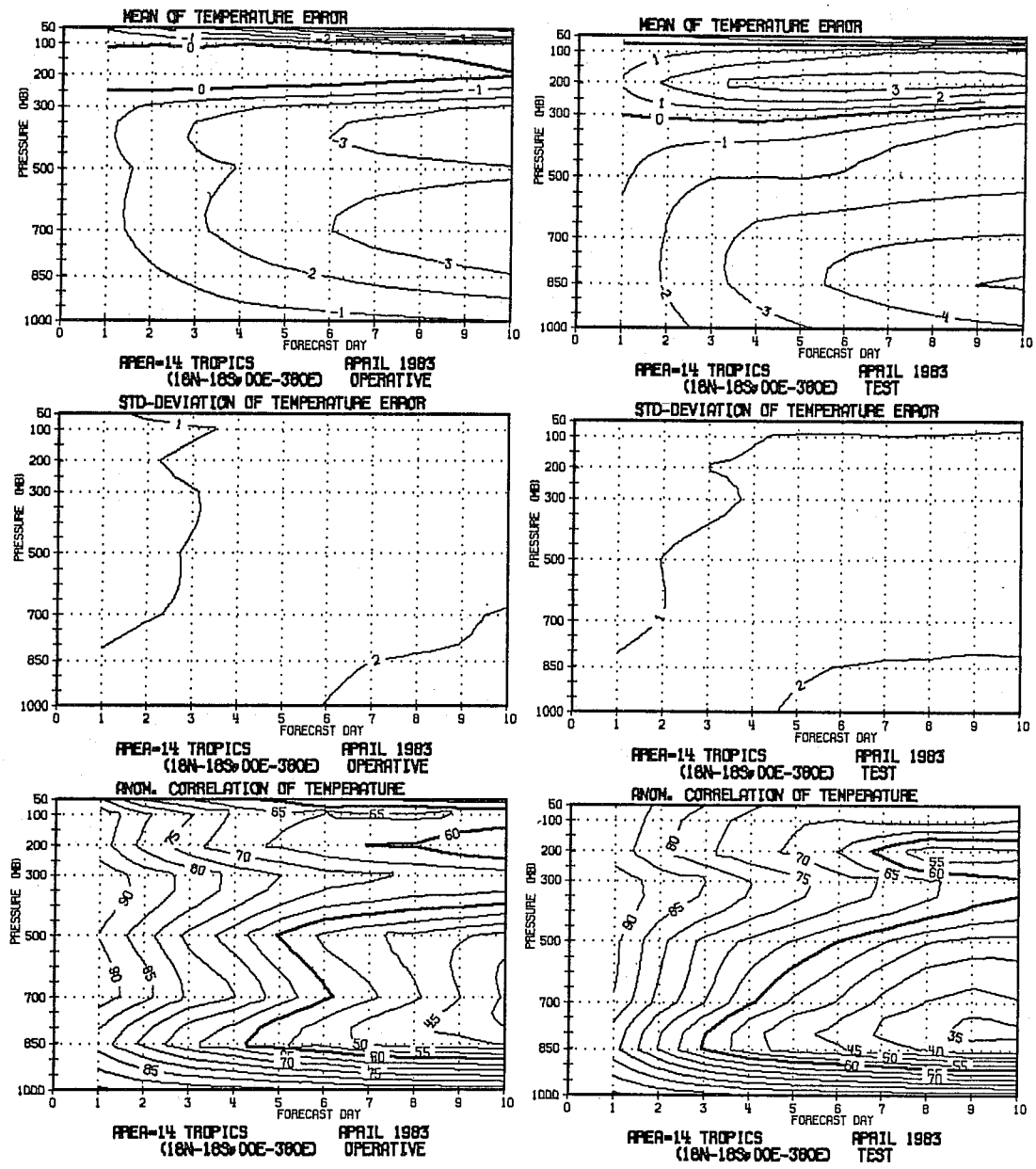

Fig. 13 As Fig. 2, for temperature over the tropical belt.

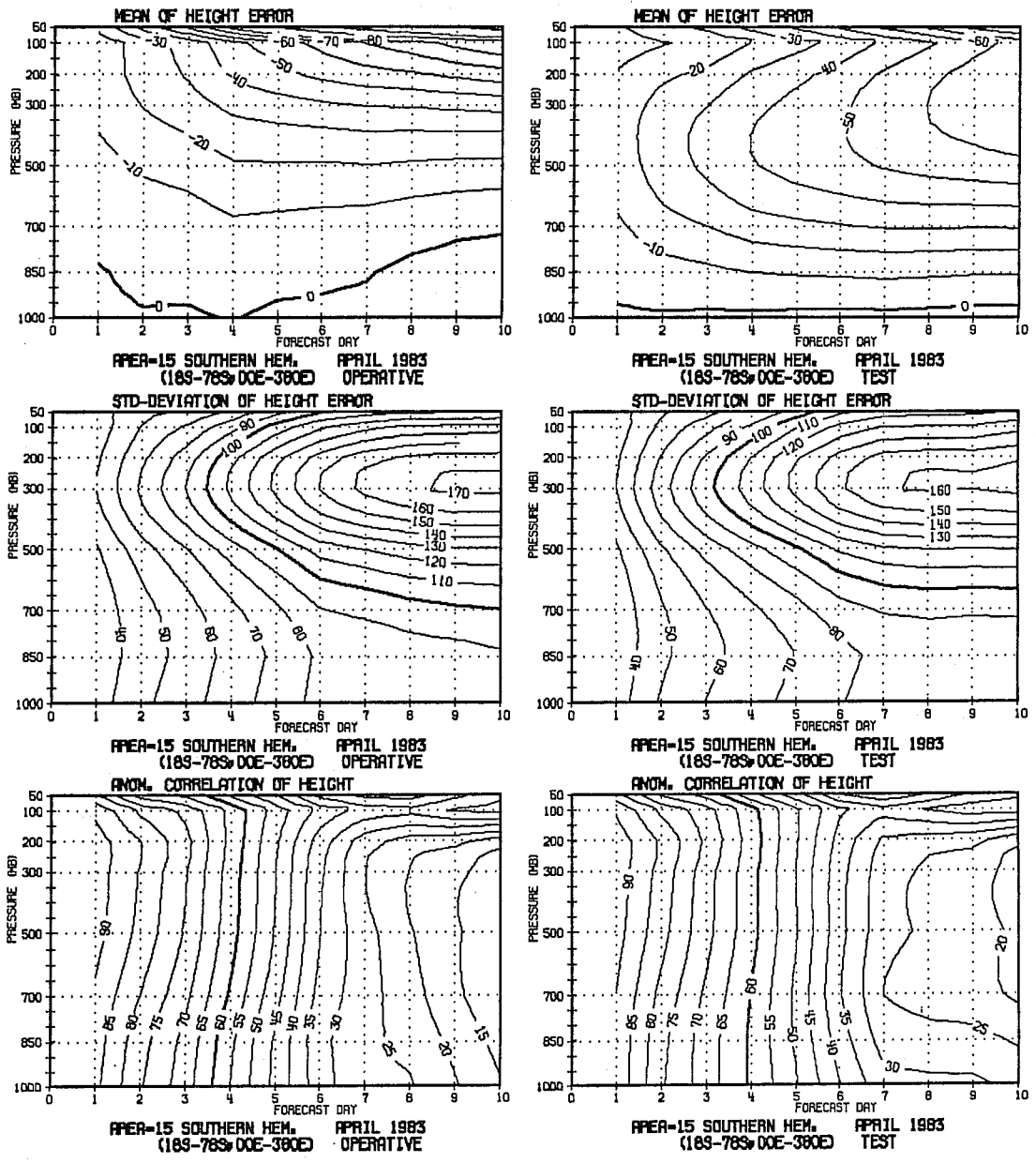

Fig. 14 As Fig. 2, for the Southern Hemisphere.

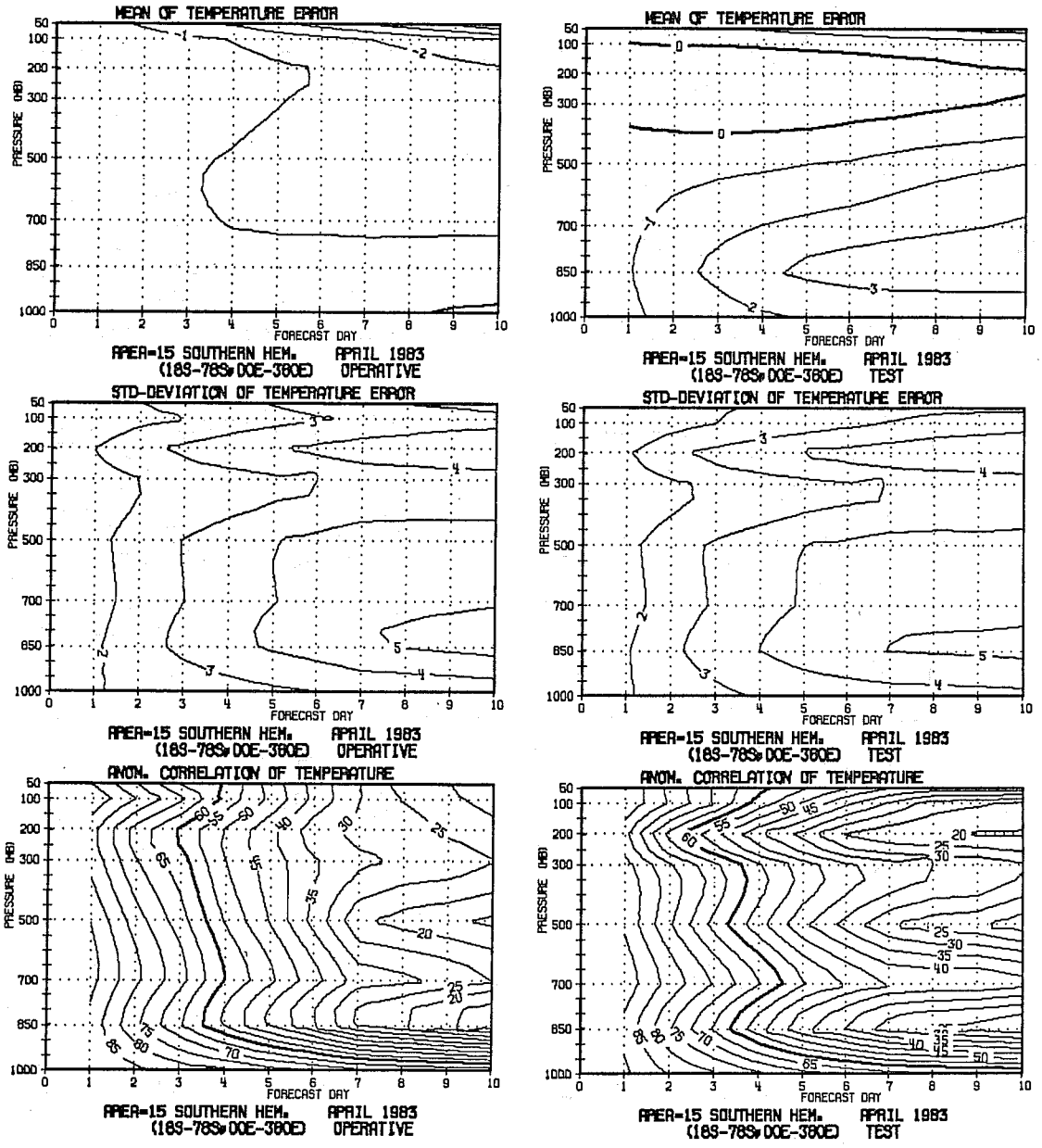

Fig. 15 As Fig. 2, for temperature over the Southern Hemisphere.

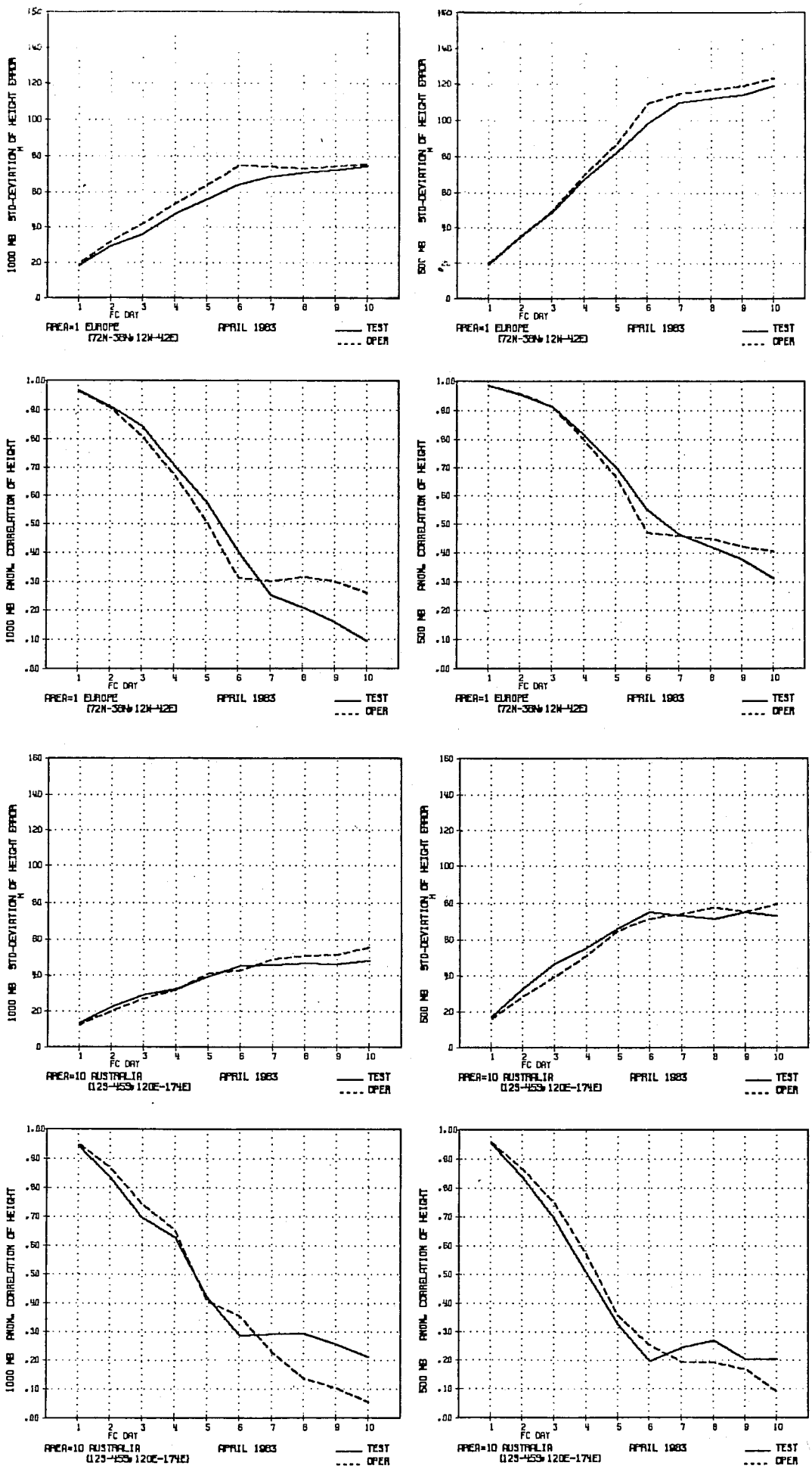

Fig. 16 Standard deviation of error and anomaly correlation of height for Europe (top) and Australia (bottom) for 1000 mb (left) and 500 mb (right). Comparison of spectral model (full) and gridpoint model (dashed), period 2 April to 20 April 1983.

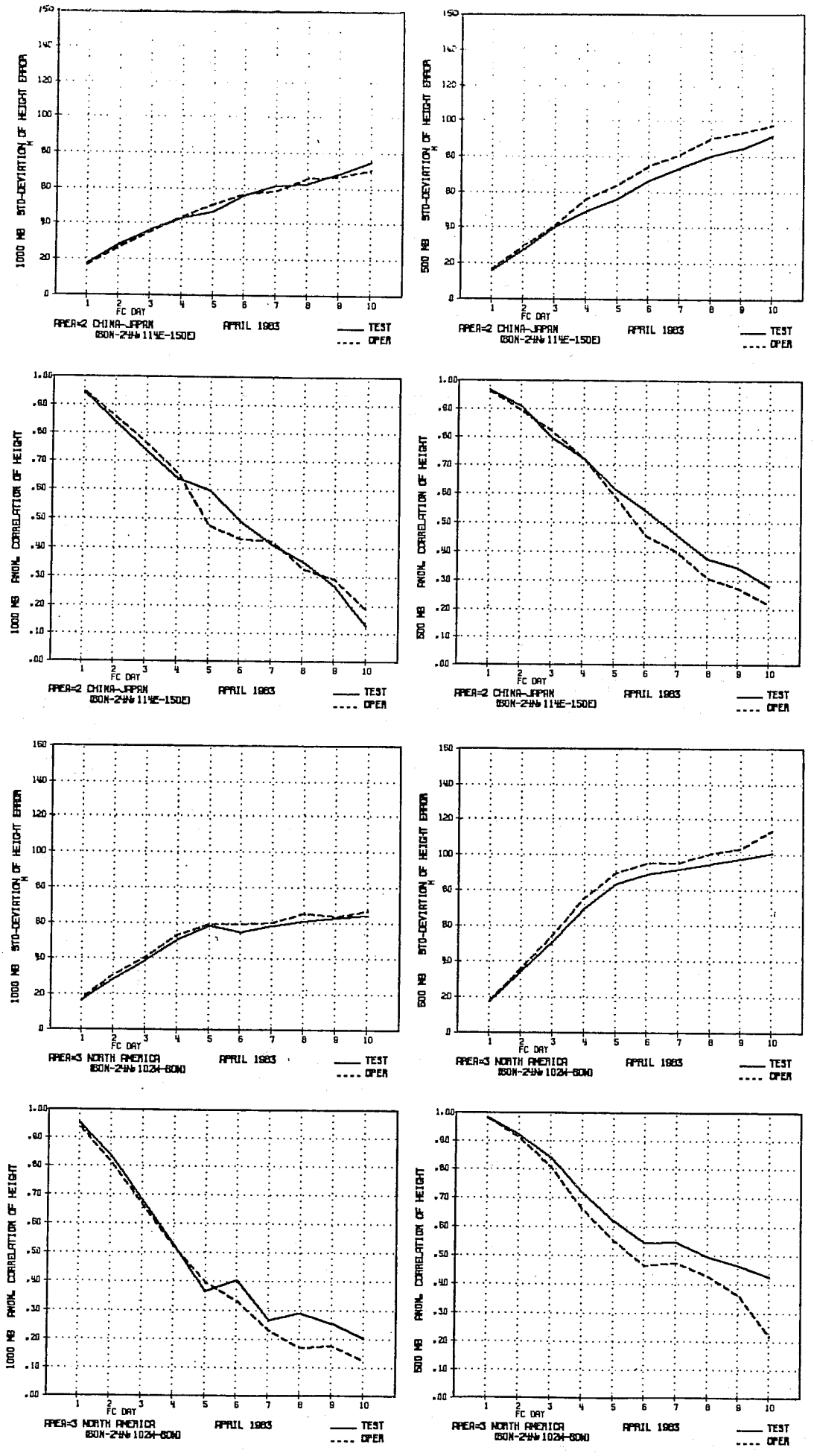

Fig. 17 As Fig. 16 for China-Japan (top) and North America (bottom).

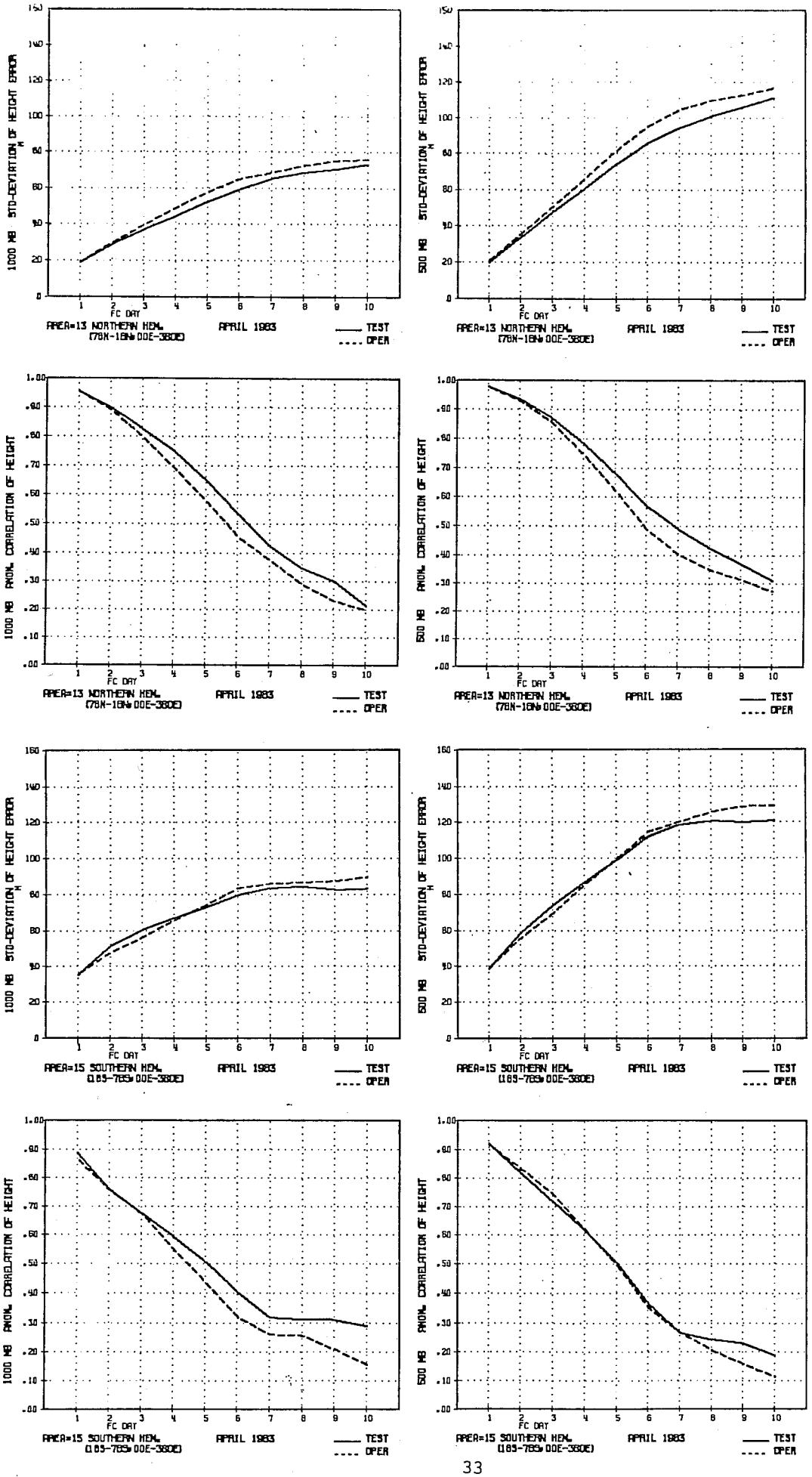

Fig. 18 As Fig. 16 for Northern Hemisphere (top)and Southern Hemisphere (bottom).

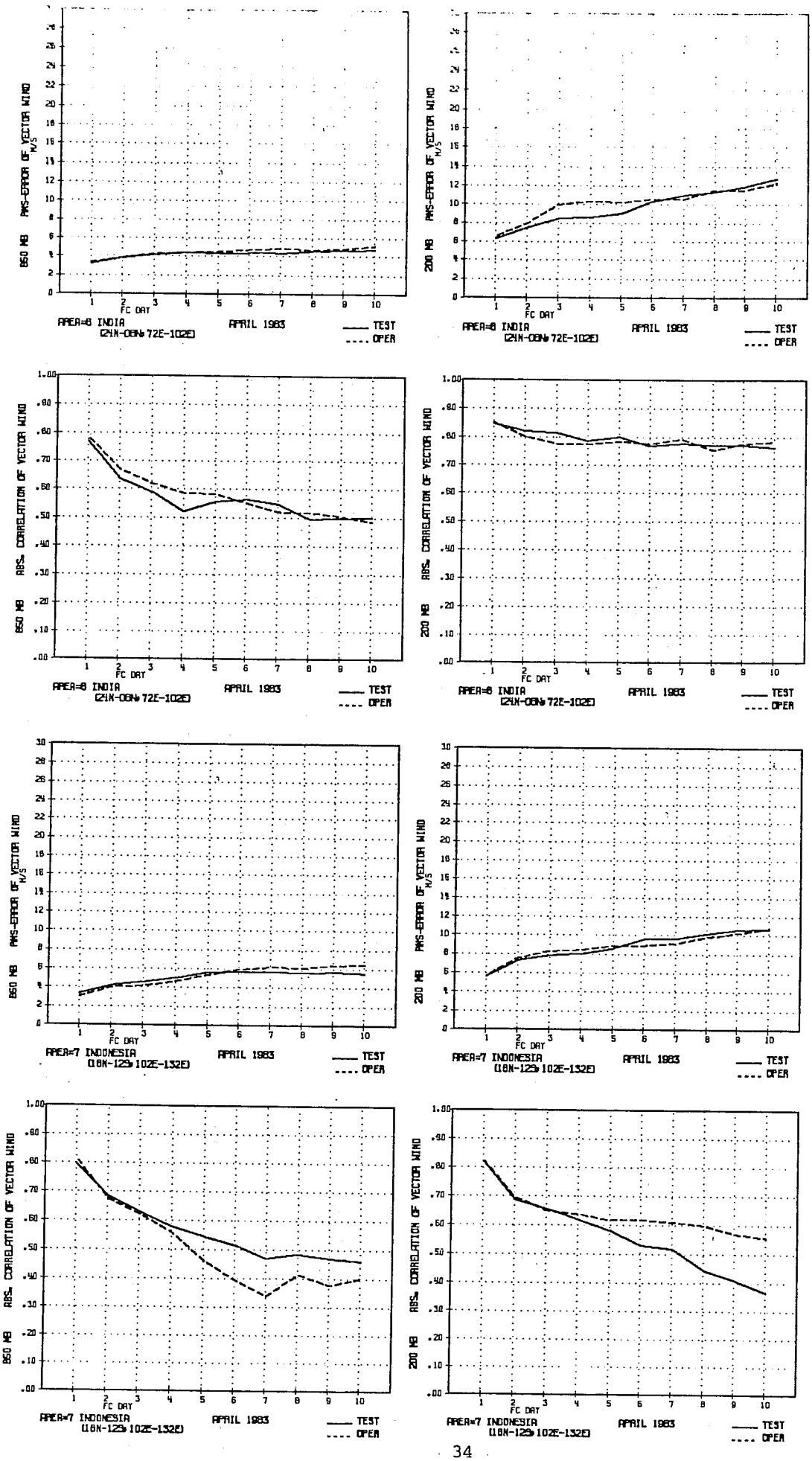

Fig. 19 As Fig. 16, RMS error and anomaly correlation of vector grid for India (top) and Indonesia (bottom).

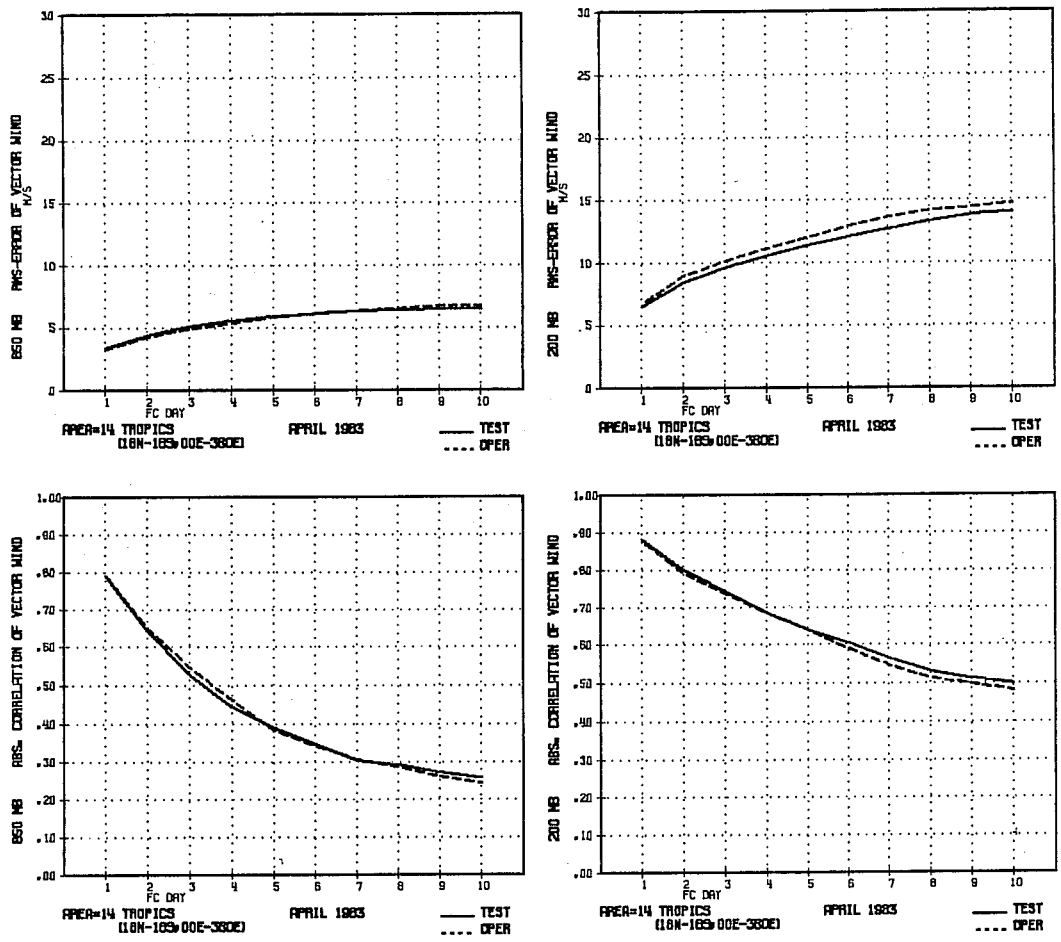

Fig. 20 As Fig. 19 for the tropical belt.

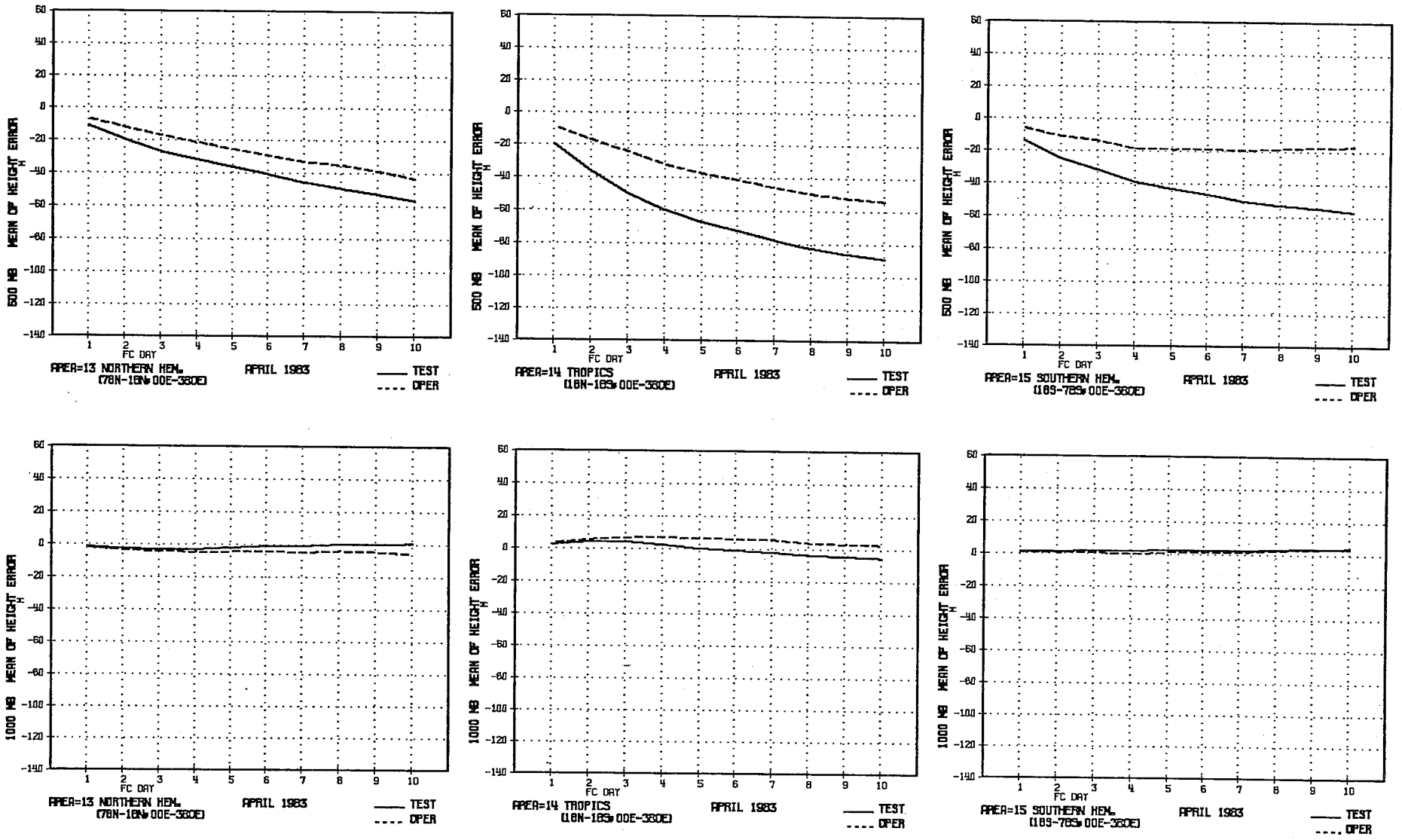

Fig. 21 1000 mb mean height error over the Northern Hemipshere, the tropical belt and the Southern Hemisphere (left to right) for the spectral model (full) and the gridpoint model (dashed), period 2-20 April 1982

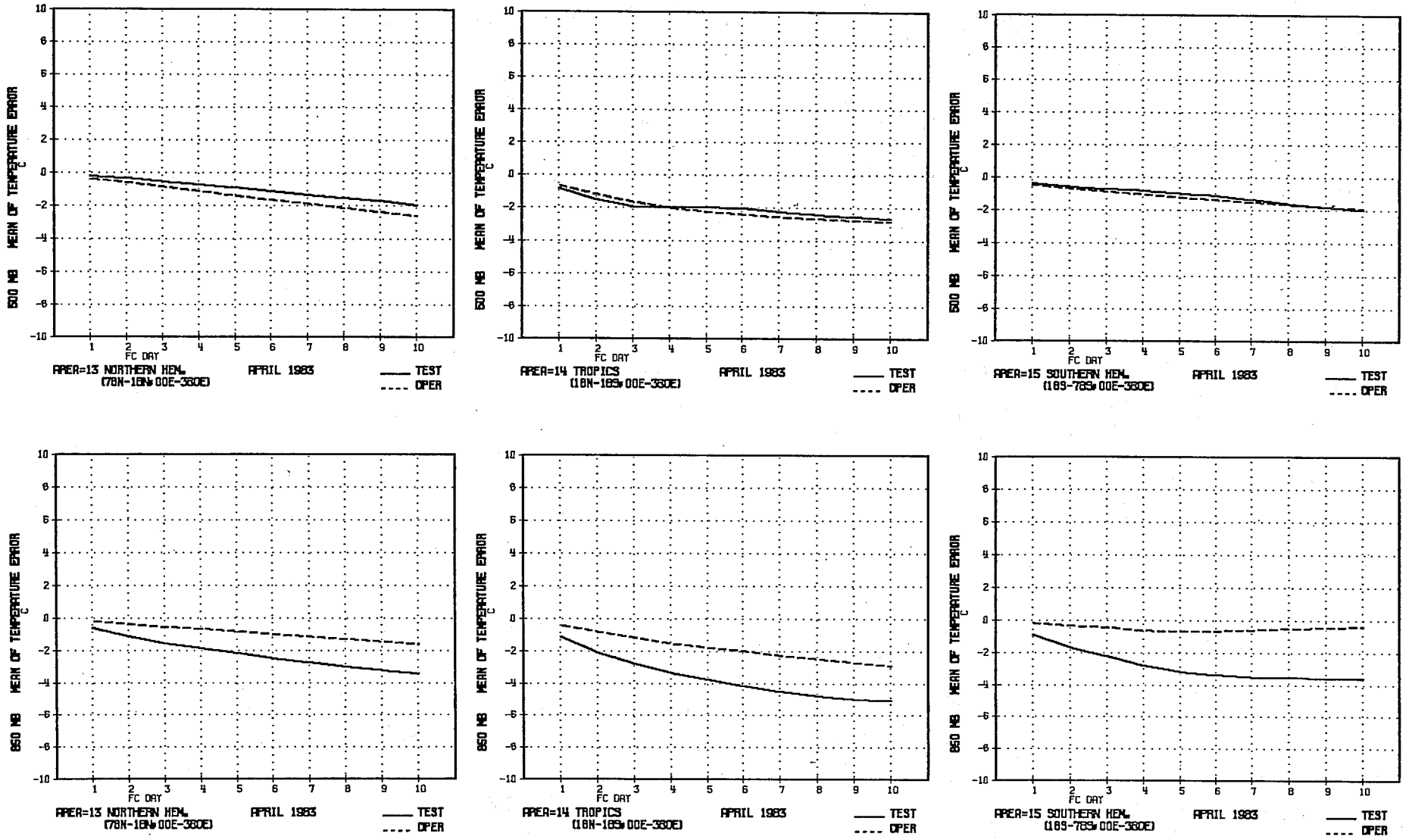

Fig. 22 As Fig. 21 for 850 mb temperature.

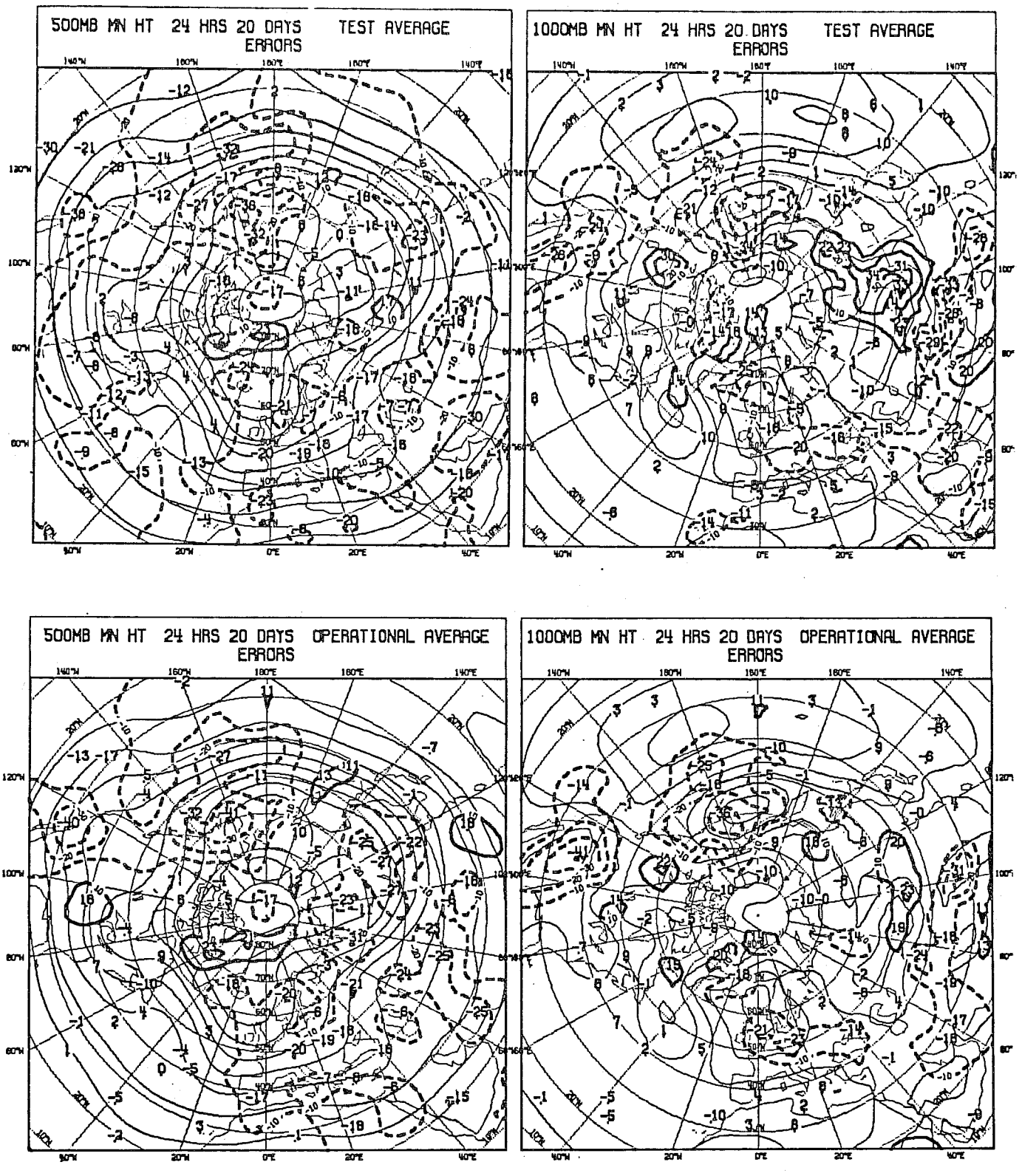

Fig. 23 Mean height error for the ensemble of 24 hour forecasts for the Northern Hemisphere

Upper left: 500mb spectral forecast
Upper right: 1000mb spectral forecast
Lower left: 500mb grid-point forecast
Lower right: 1000mb grid-point forecast
Units in m, contour interval: 10m

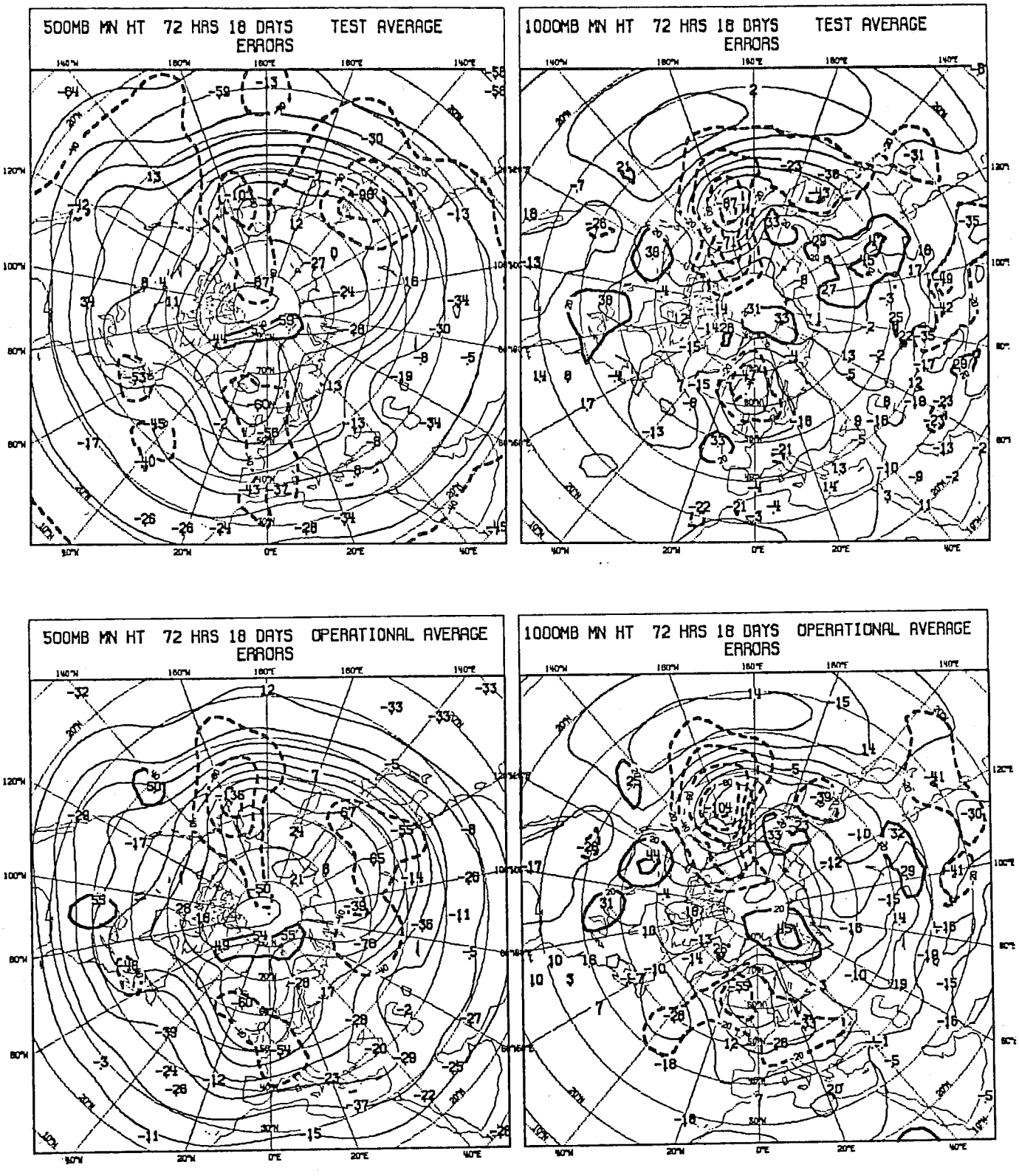

Fig. 24 Same as Fig. 23 but for 72 hour forecasts
Contour interval: 40m for 500mb forecasts, 20m for 1000mb forecasts

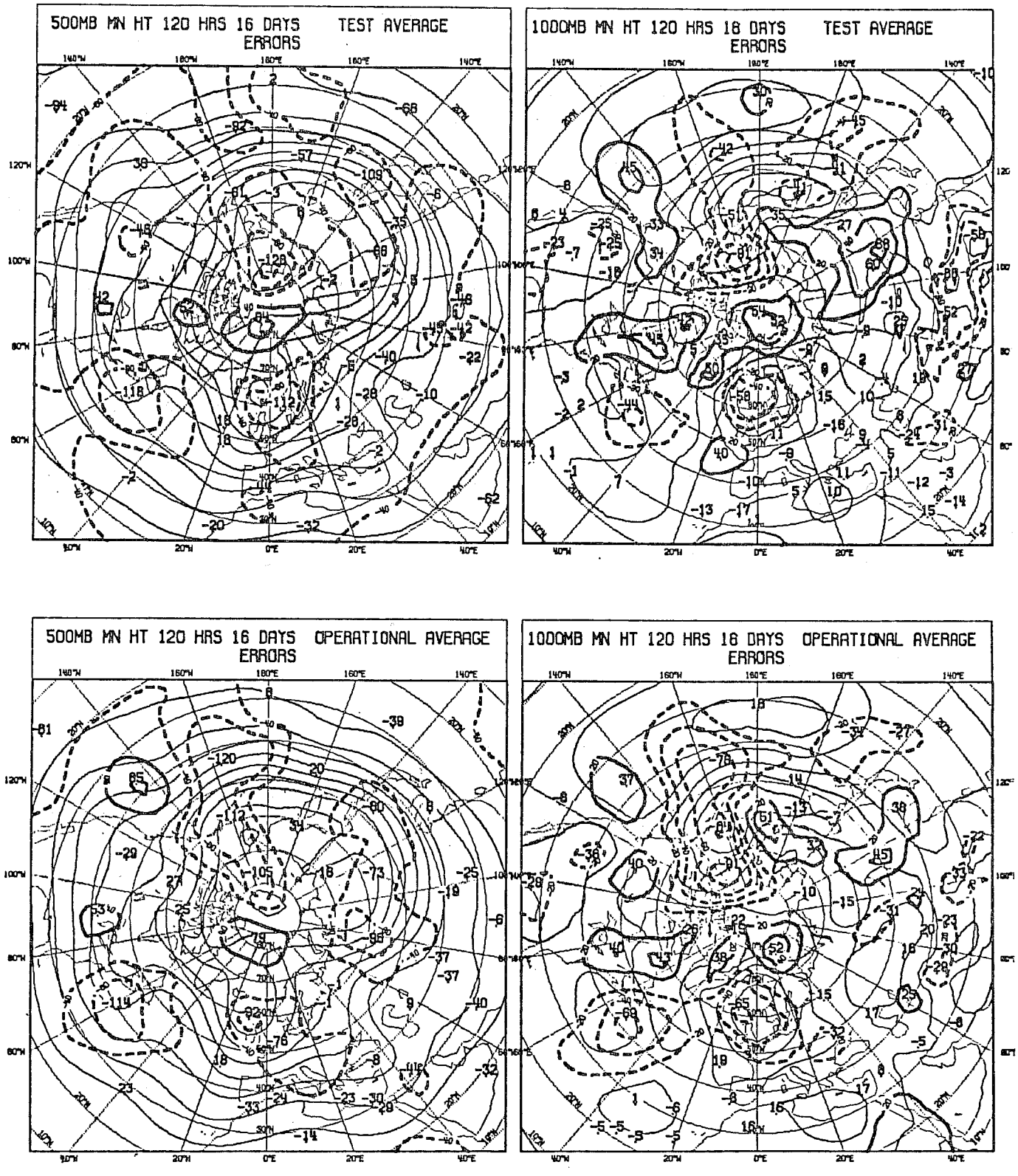

Fig. 25 Same as Fig. 24 but for 120 hour forecasts

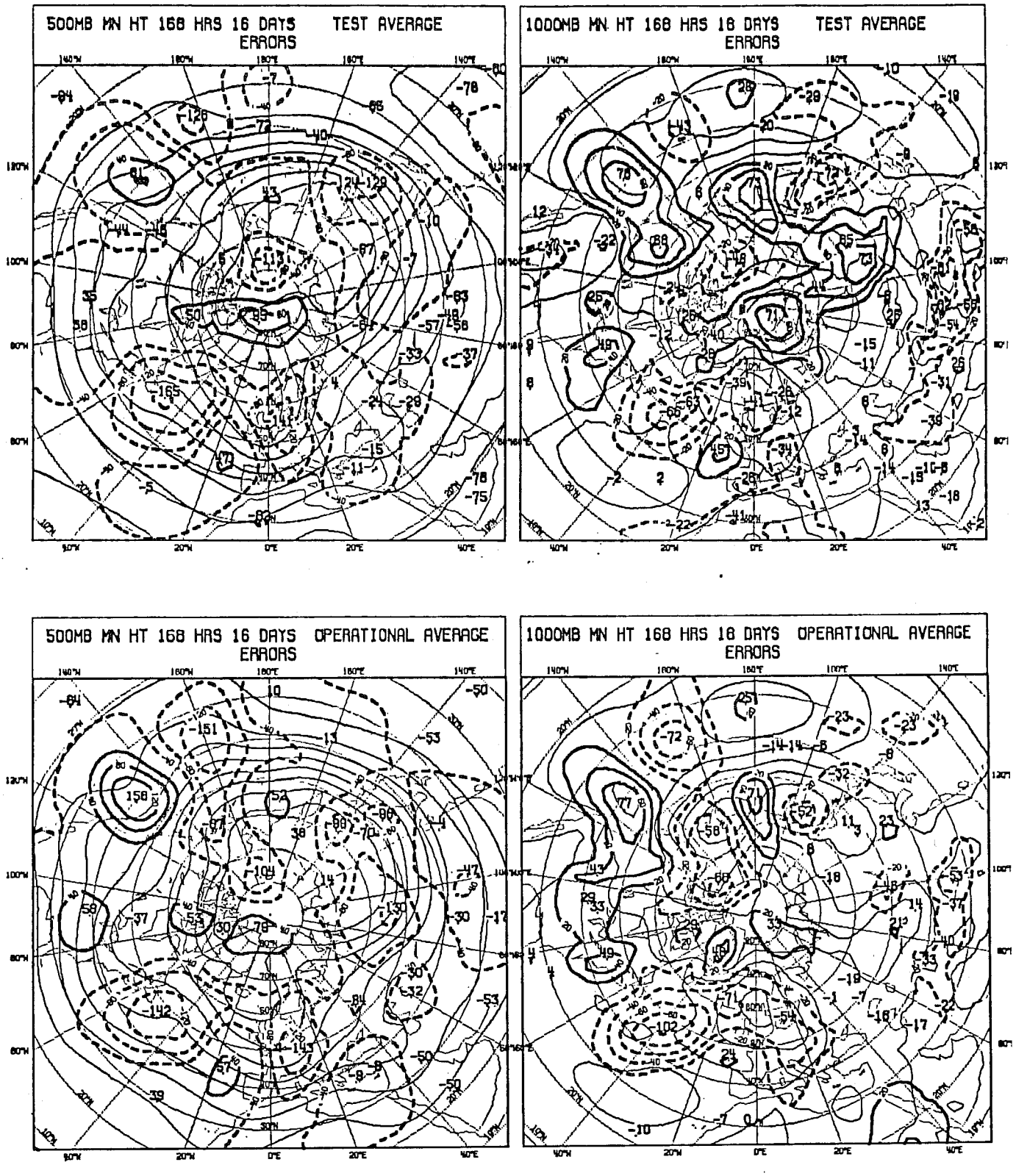

Fig. 26 Same as Fig. 24 but for 168 hour forecasts

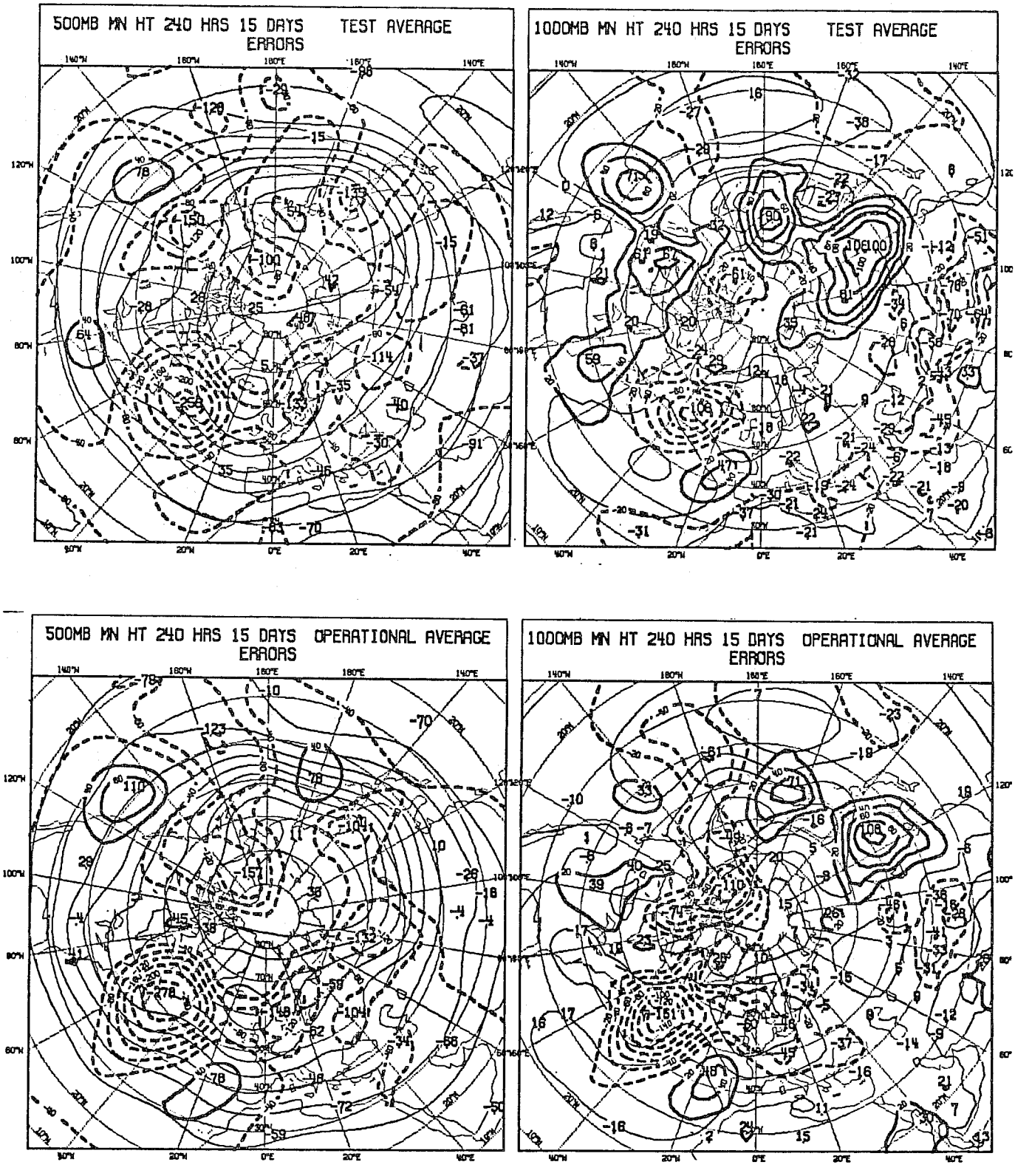

Fig. 27 Same as Fig. 24 but for 240 hour forecasts

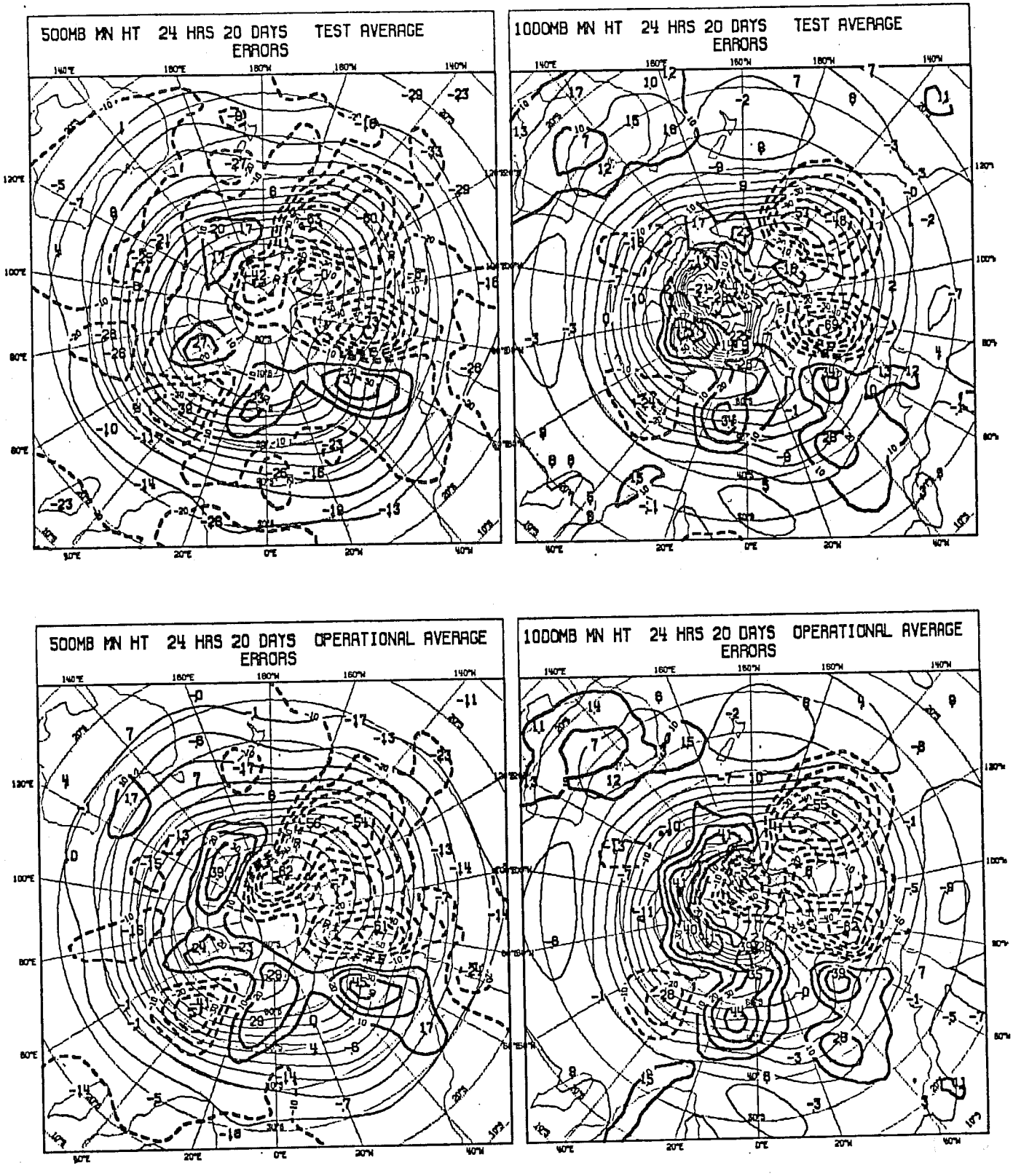

Fig. 28 Same as Fig. 23 but for the Southern Hemisphere

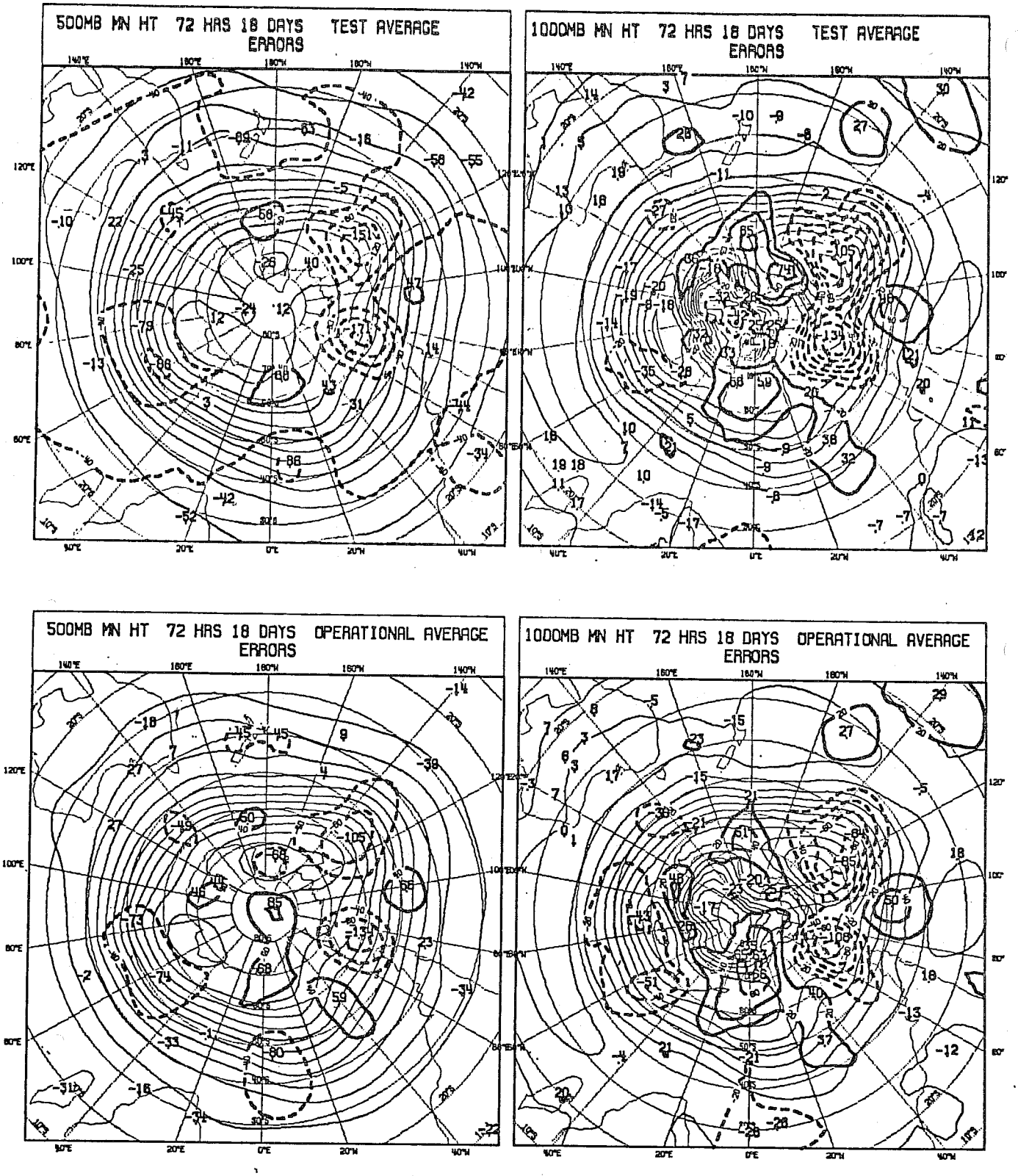

Fig. 29 Same as Fig. 24 but for the Southern Hemisphere

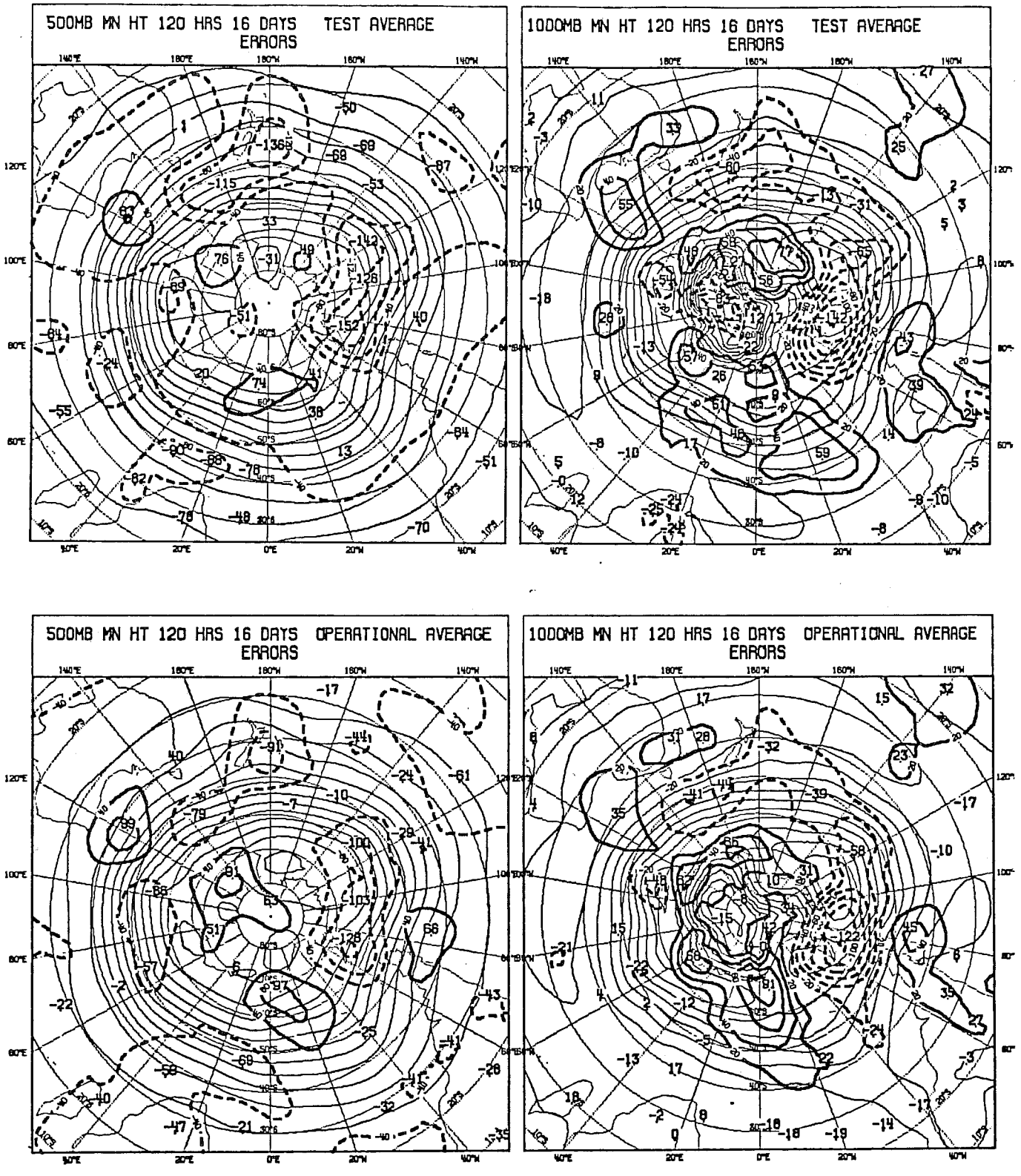

Fig. 30 Same as Fig. 25 but for the Southern Hemisphere

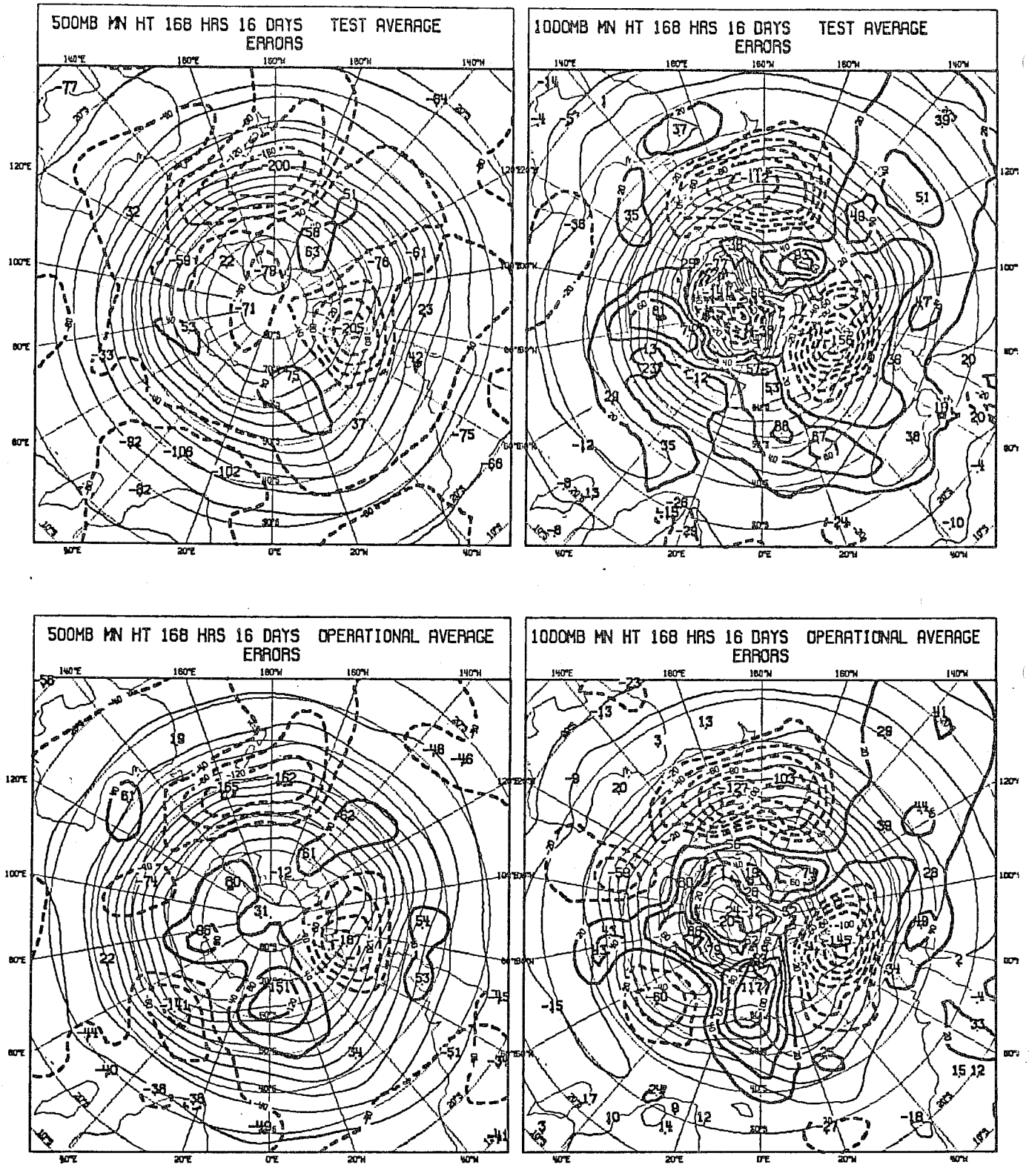

Fig. 31 Same as Fig. 26 but for the Southern Hemisphere

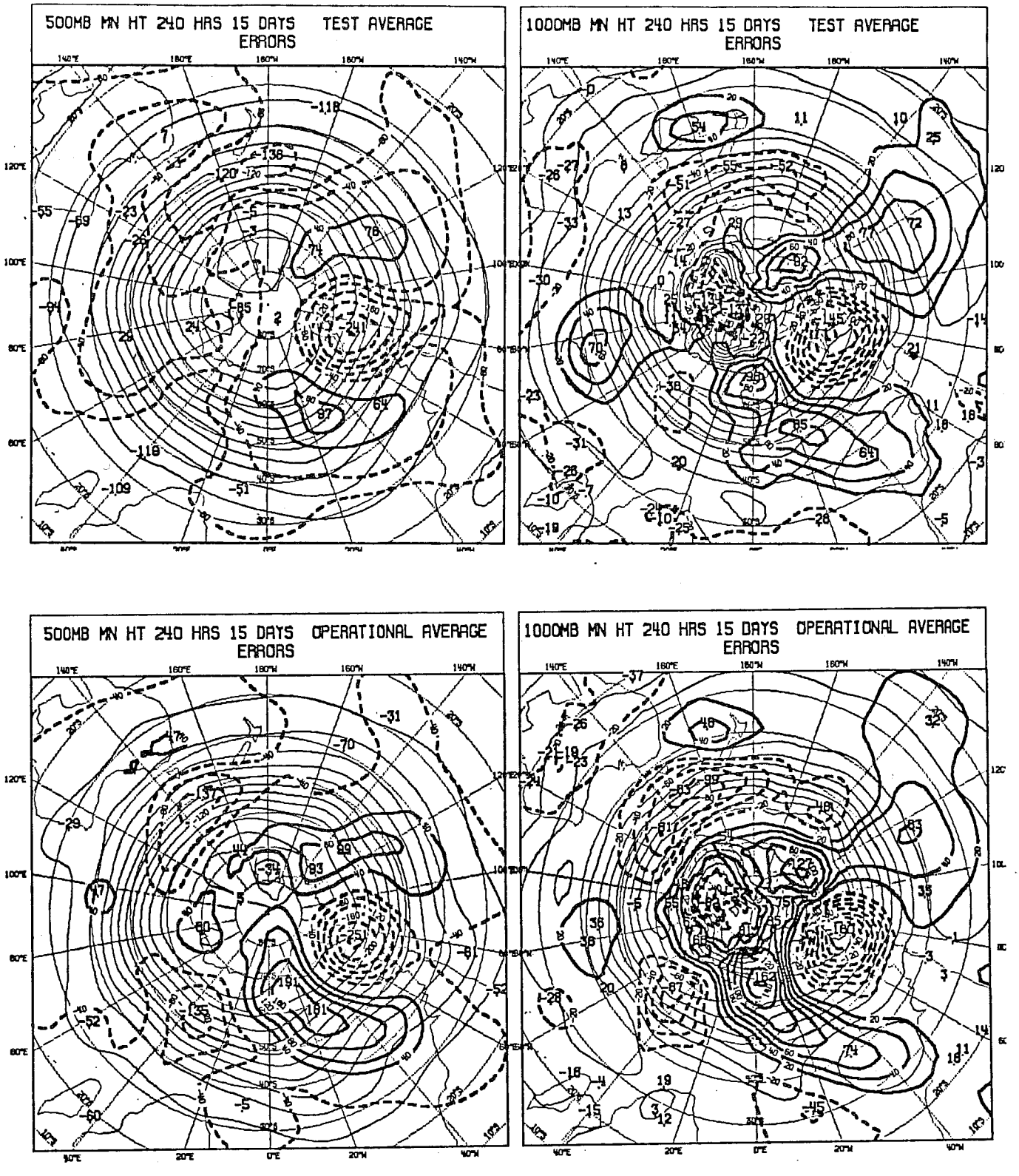

Fig. 32 Same as Fig. 27 but for the Southern Hemisphere

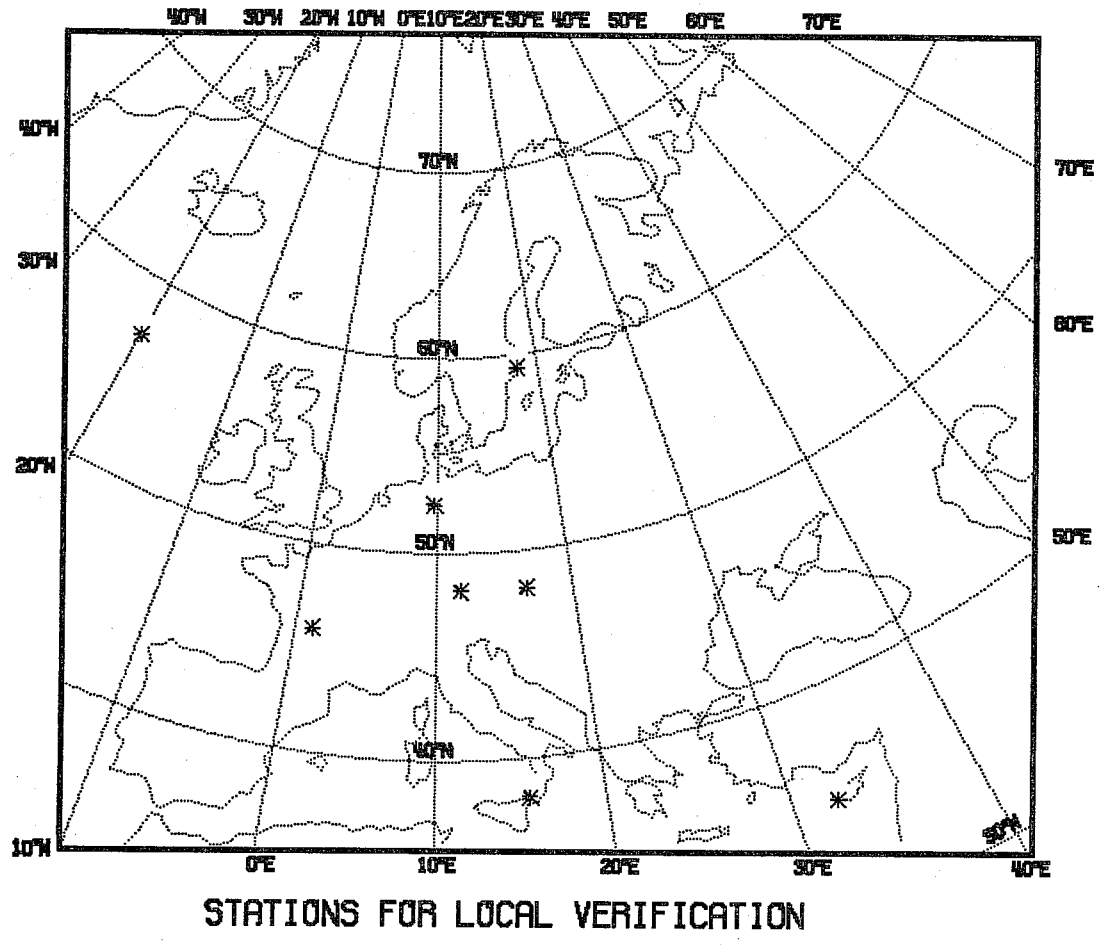

Fig. 33 Locations of stations used in verification of surface weather parameters.

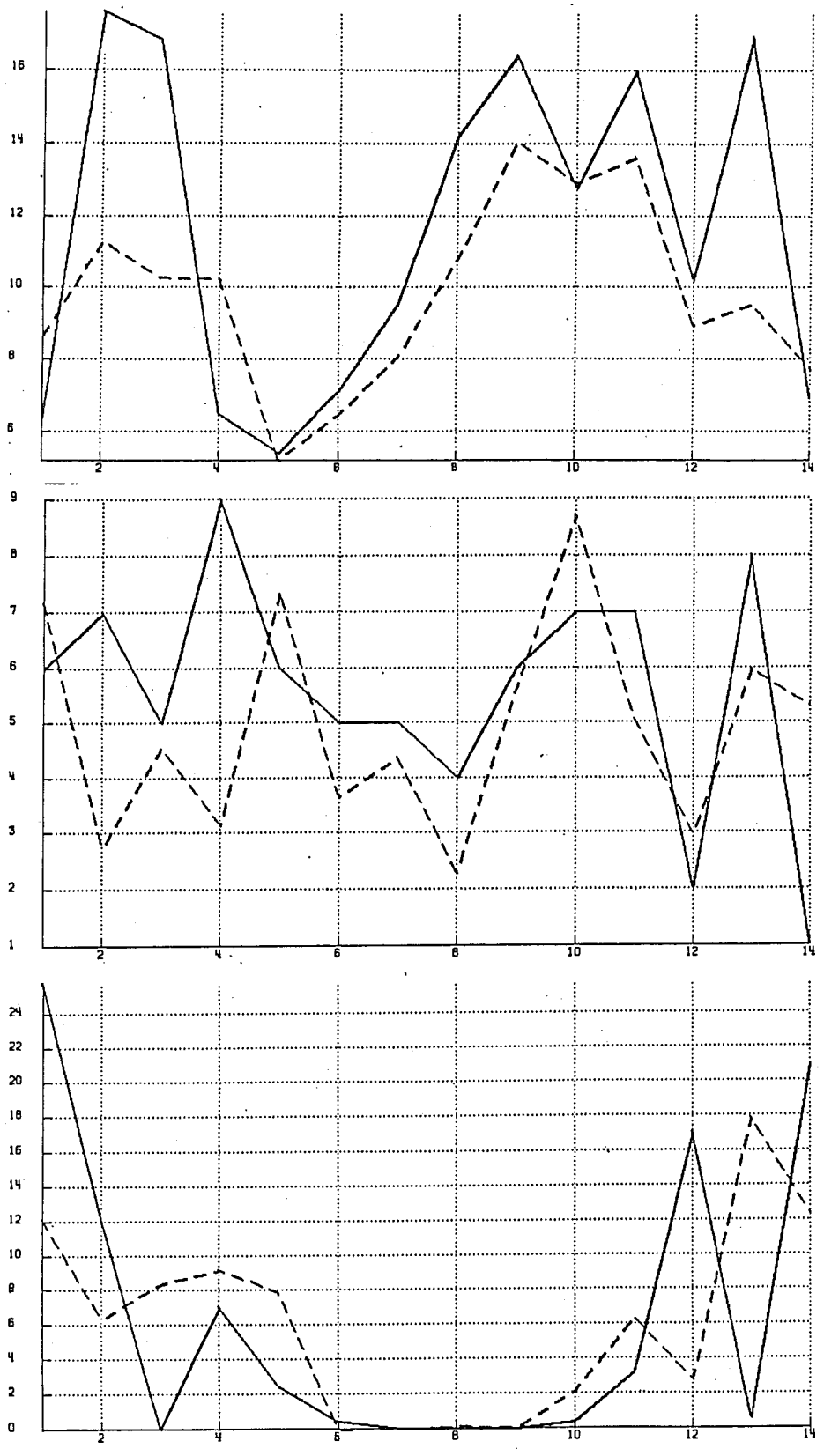

Fig. 34 Verification of near surface parameters at Limoges for temperature at 2m, windspeed at 10m and precipitation amount (from top to bottom). Full line is the observation, dashed line is the 48 hour forecast from the operational gridpoint model. Period 2-18 April 1983.

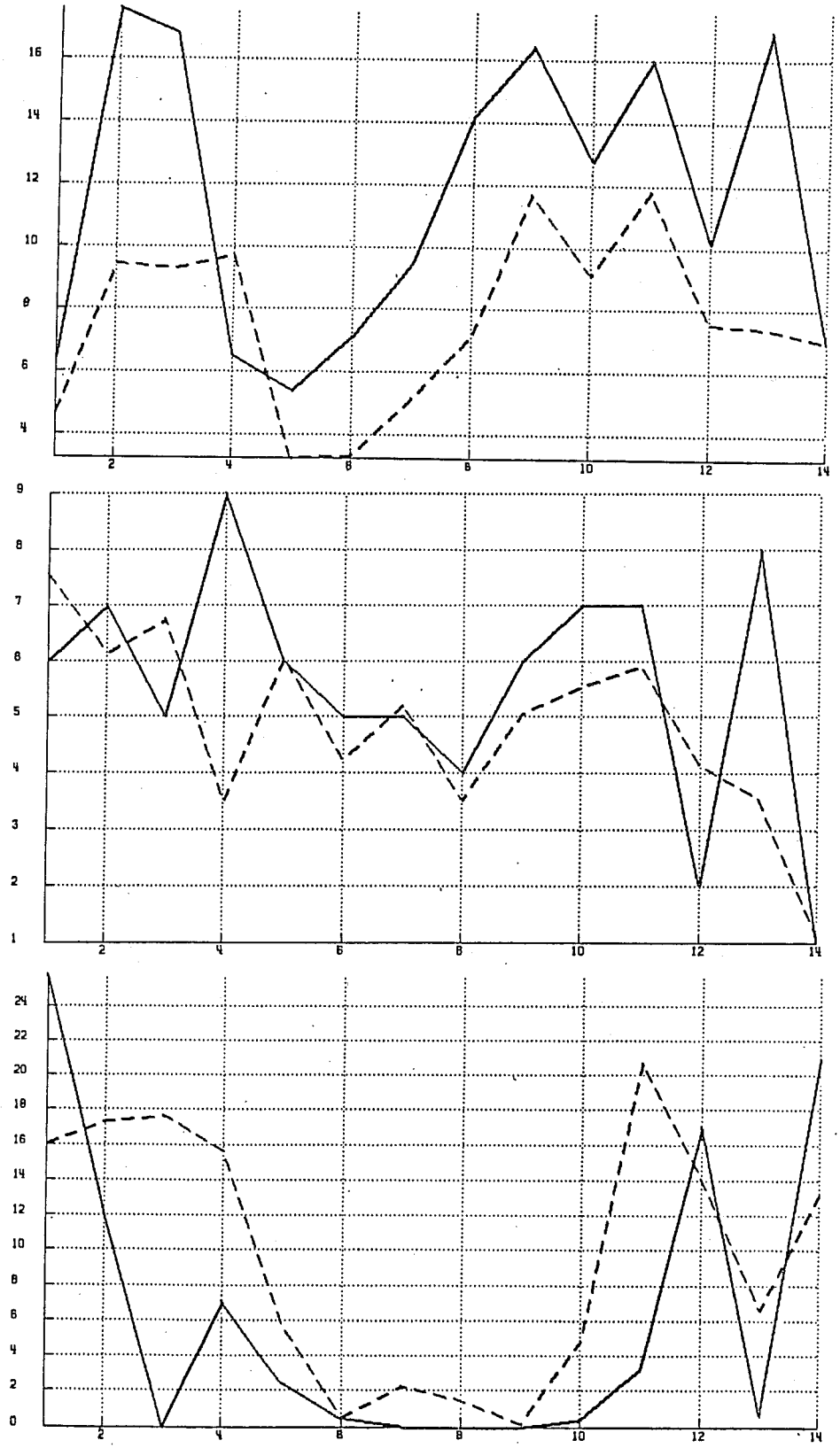

Fig. 35 Same as Fig. 34, dashed line gives the 48 hr forecast from the spectral model.

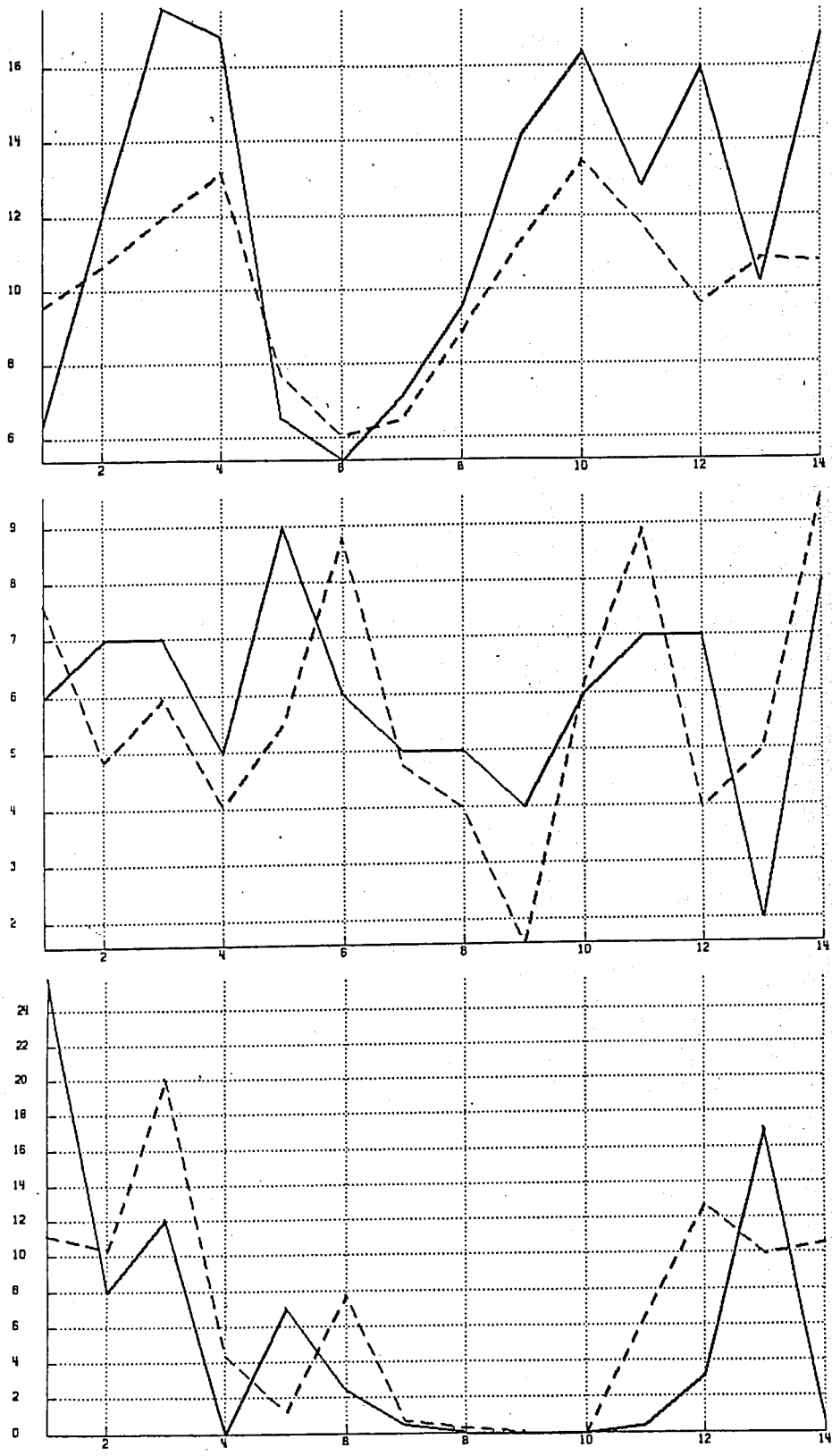

Fig. 36 Verification of near surface parameters at Limoges for temperature at 2m, windspeed at 10m and precipitation amount (from top to bottom). Full line is the observation, dashed line is the 72 hour forecast from the operational gridpoint model. Period 2-18 April 1983.

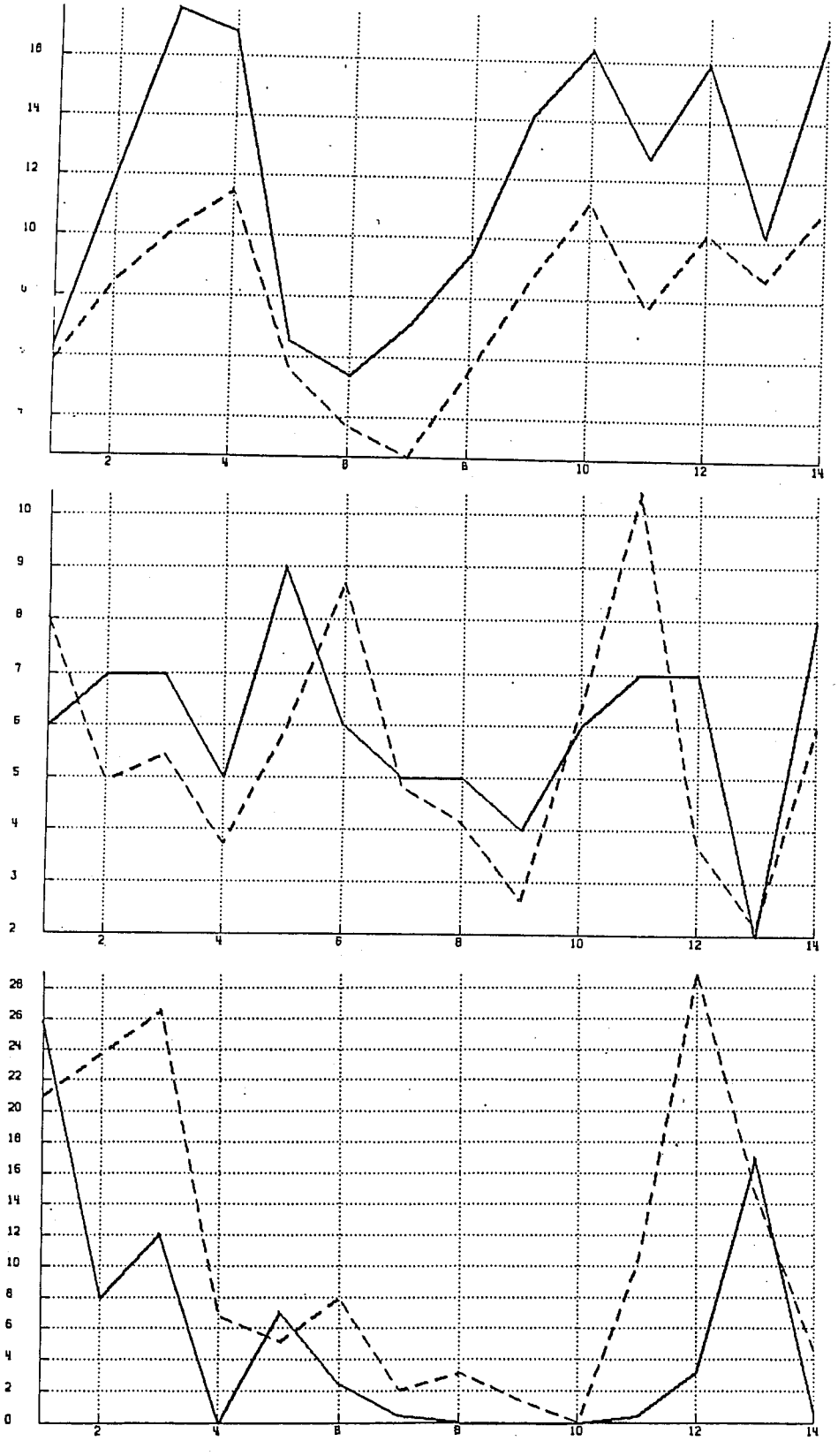

Fig. 37 Same as Fig. 36, dashed line gives the 72 hour forecast from the spectral model.

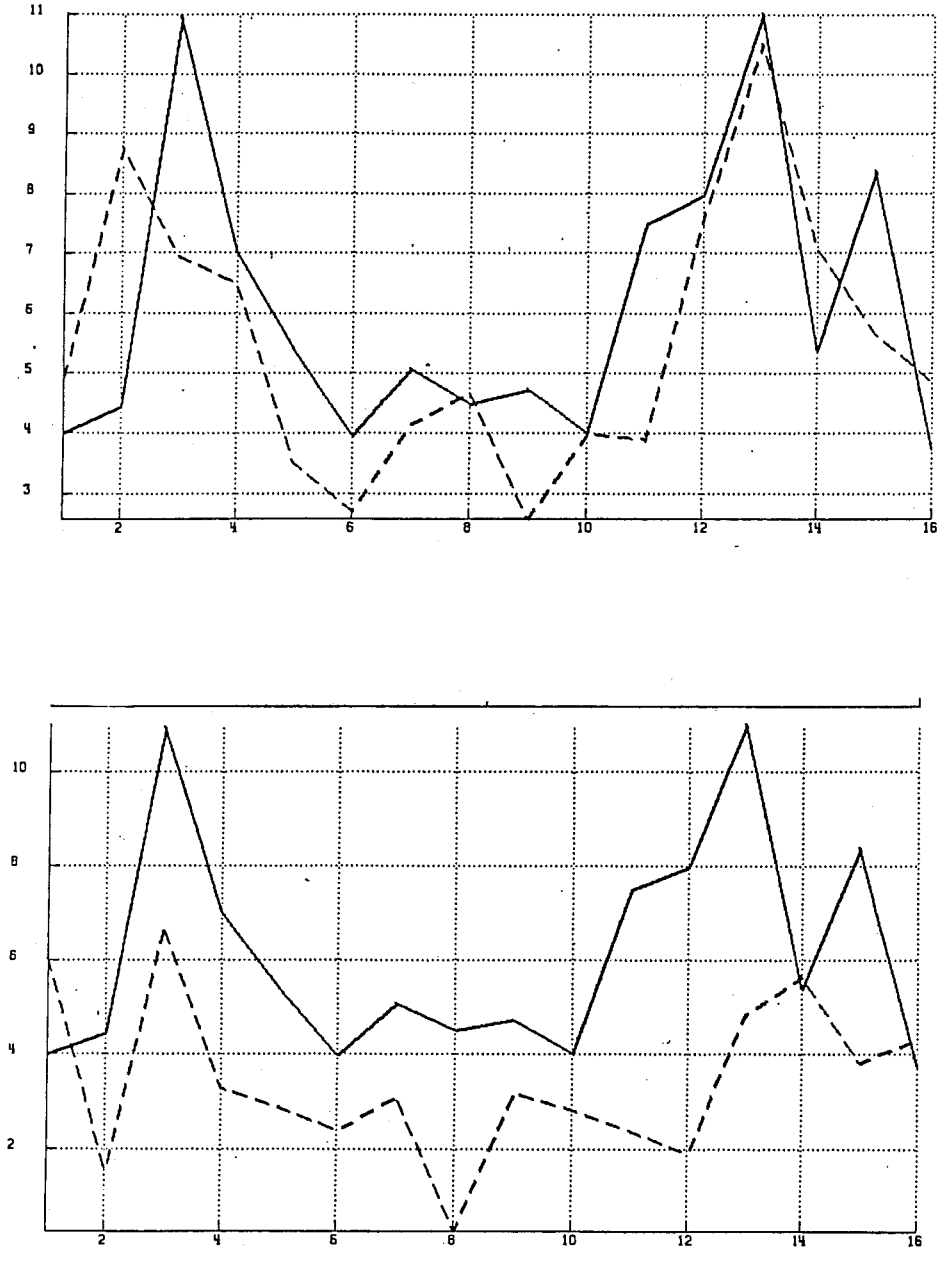

Fig. 38 Verification of 72 hour forecast of windspeed (10m) at Cyprus. Full line is the observation, dashed line the forecast, top panel gives the result from the gridpoint model and the bottom panel the verification for the spectral model forecast, period 2-18 April 1983.

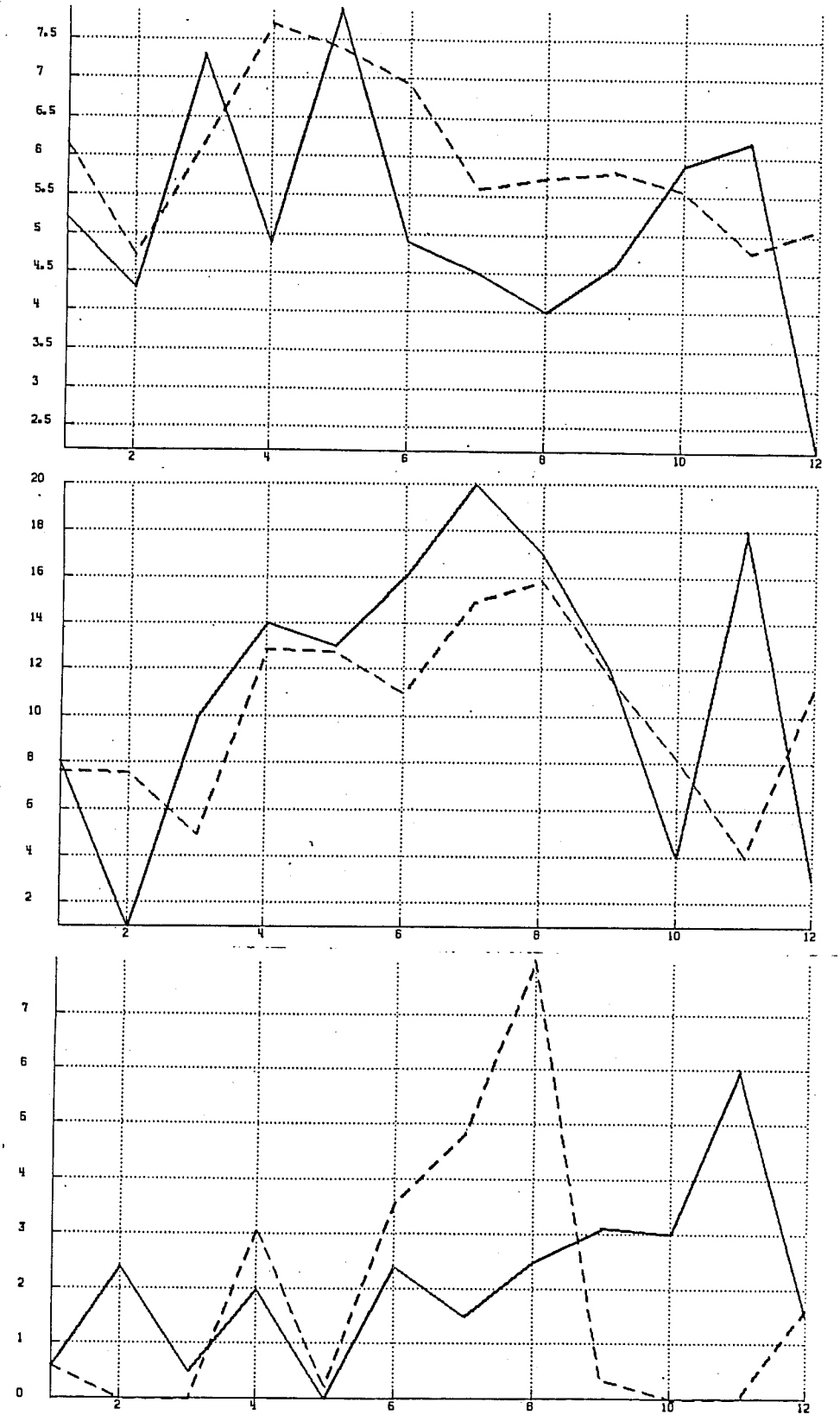

Fig. 39 Verification of near surface parameters at OWS Lima for temperature at 2m, windspeed at 10m and precipitation amount (from top to bottom). Full line is the observation, dashed line is the 72 hour forecast from the operational gridpoint model. Period 2-18 April 1983.

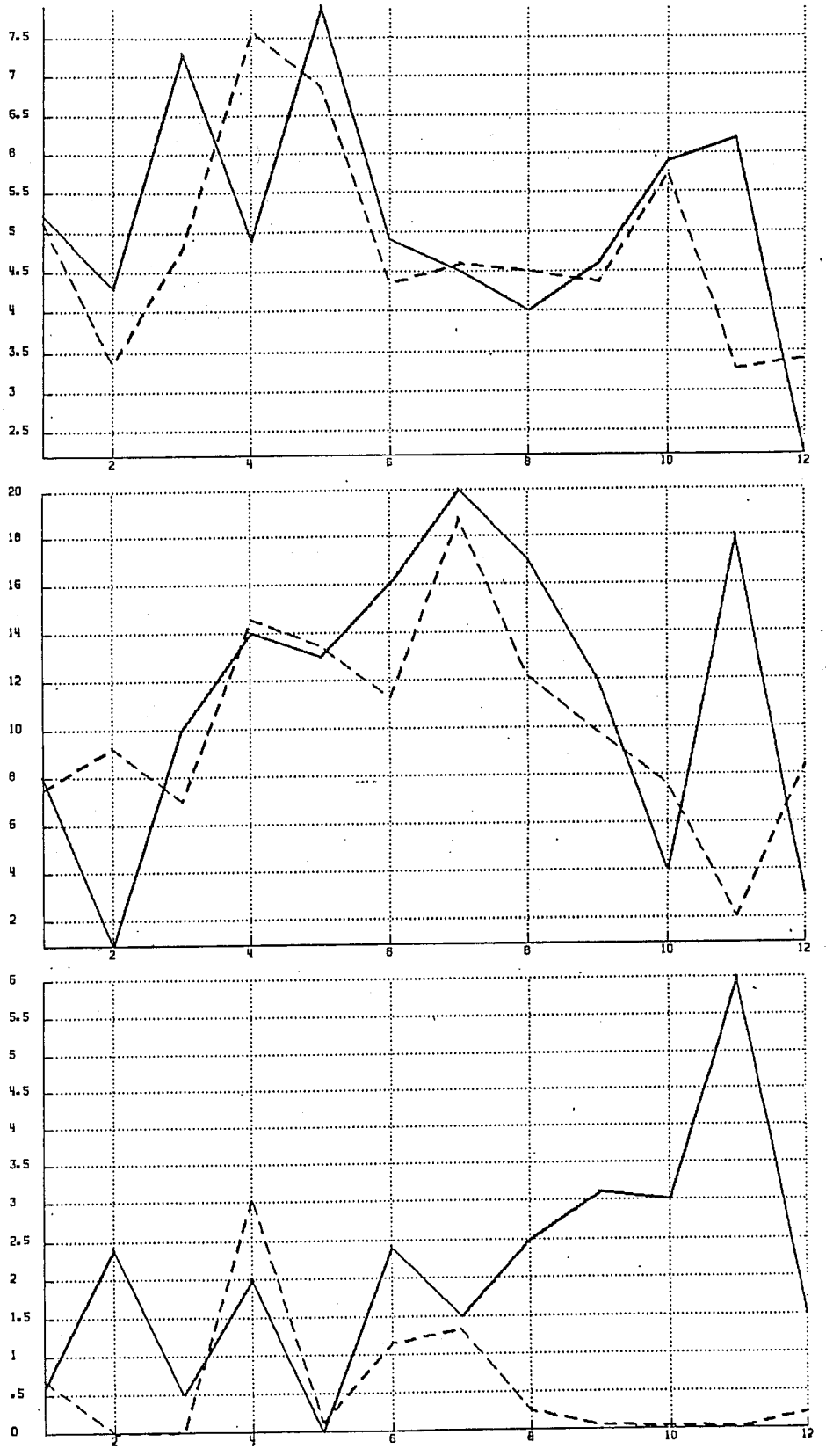

Fig. 40 Same as Fig. 39, dashed lines give the 72 hour forecast from the spectral model.

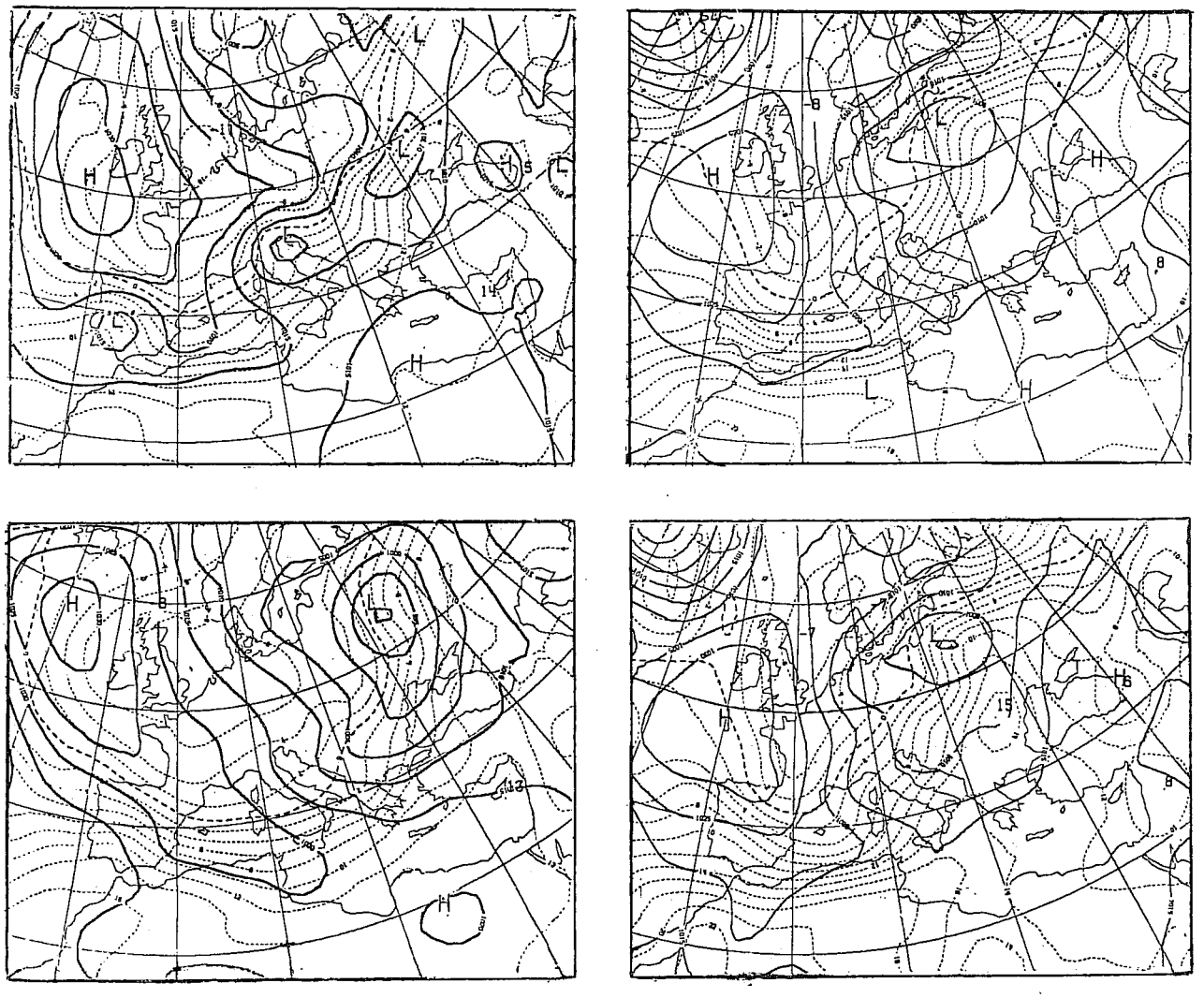

Fig. 41 1000mb height (solid) and 850mb temperature (dashed) fields

Upper left: 120 hour spectral forecast from 7 April 1983
Lower left: 120 hour grid-point forecast from 7 April 1983
Upper right: Spectral model analysis at 12 GMT 12 April 1983
Lower right: Grid-point model analysis at 12 GMT 12 April 1983

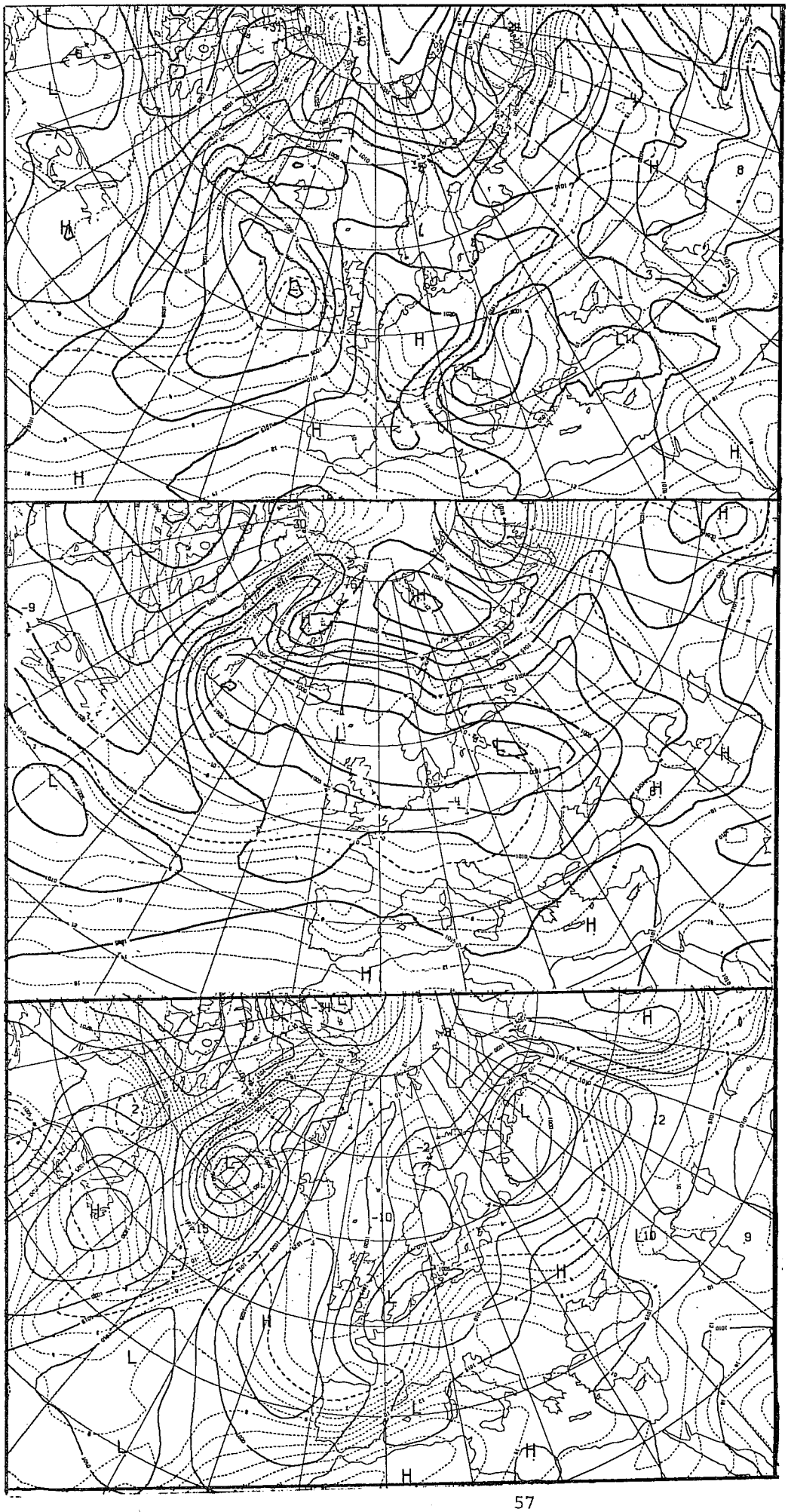

Fig. 42

1000mb height and 850mb temperature D+8 spectral forecast (top), D+8 grid-point forecast (middle), and analysis (bottom) all valid at 12 GMT 11 April 1983.

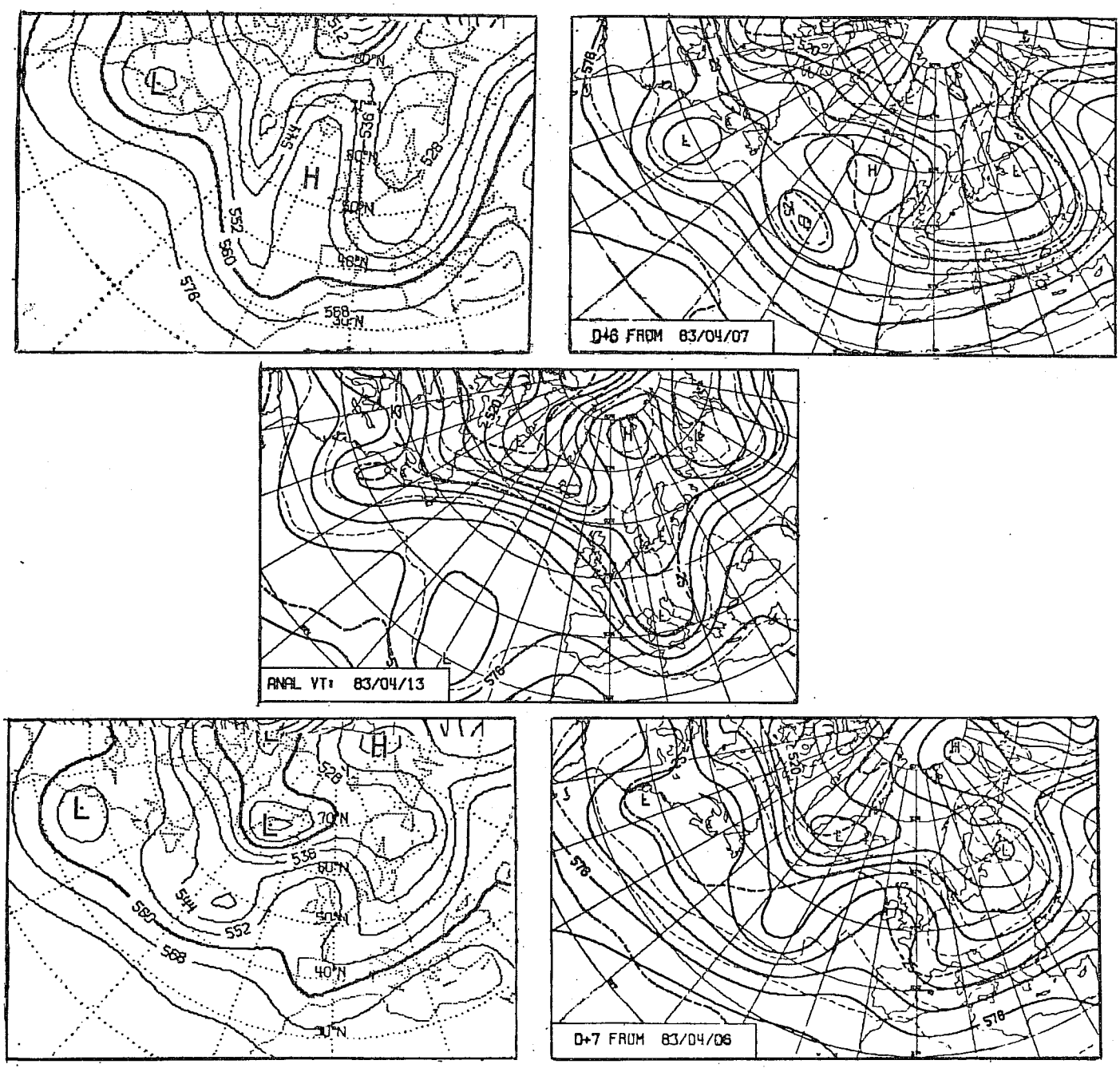

Fig. 43 500mb forecasts (top and bottom row) and analysis (middle row) of geopotential height, valid time 12 GMT 13 April 1983. The upper left frame shows the 144 hour spectral forecast from 7 April 1983, the upper right the corresponding grid-point forecast. The lower left frame shows the 168 hour spectral forecast from 6 April 1983, the lower right the corresponding grid-point forecast.

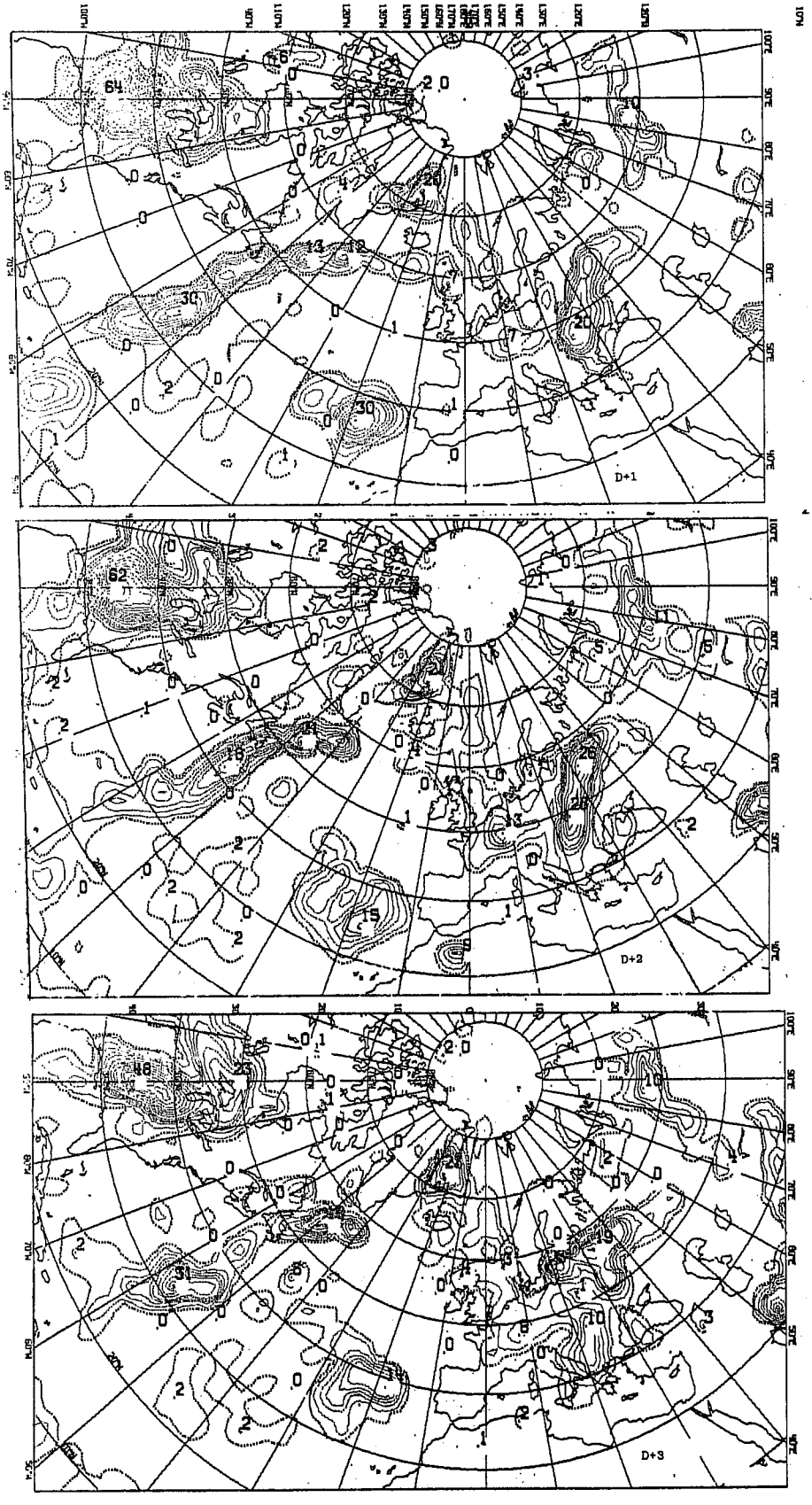

Fig. 44 Precipitation accumulated from the spectral model during the period 12 GMT 13 April - 12 GMT 14 April 1983. (Unit: mm).
Top: 24 hour forecast from 13 April 1983
Middle: 48 hour forecast from 12 April 1983
Bottom: 72 hour forecast from 11 April 1983

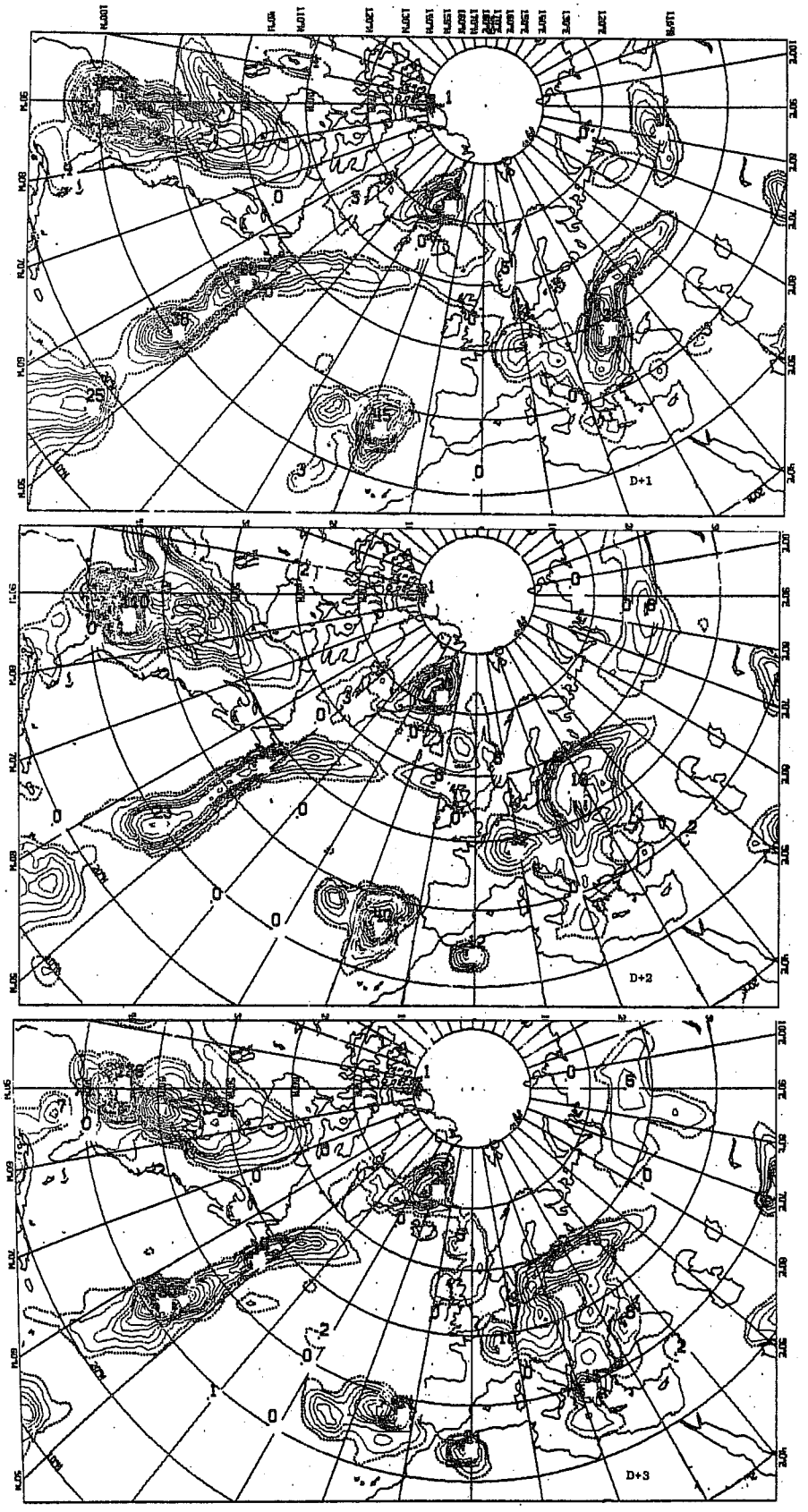

Fig. 45 Precipitation accumulated from the grid-point model during the period 00 GMT 14 April - 00 GMT 15 April 1983. (Unit: mm).
Top: 36 hour forecast from 13 April 1983
Middle: 60 hour forecast from 12 April 1983
Bottom: 84 hour forecast from 11 April 1983

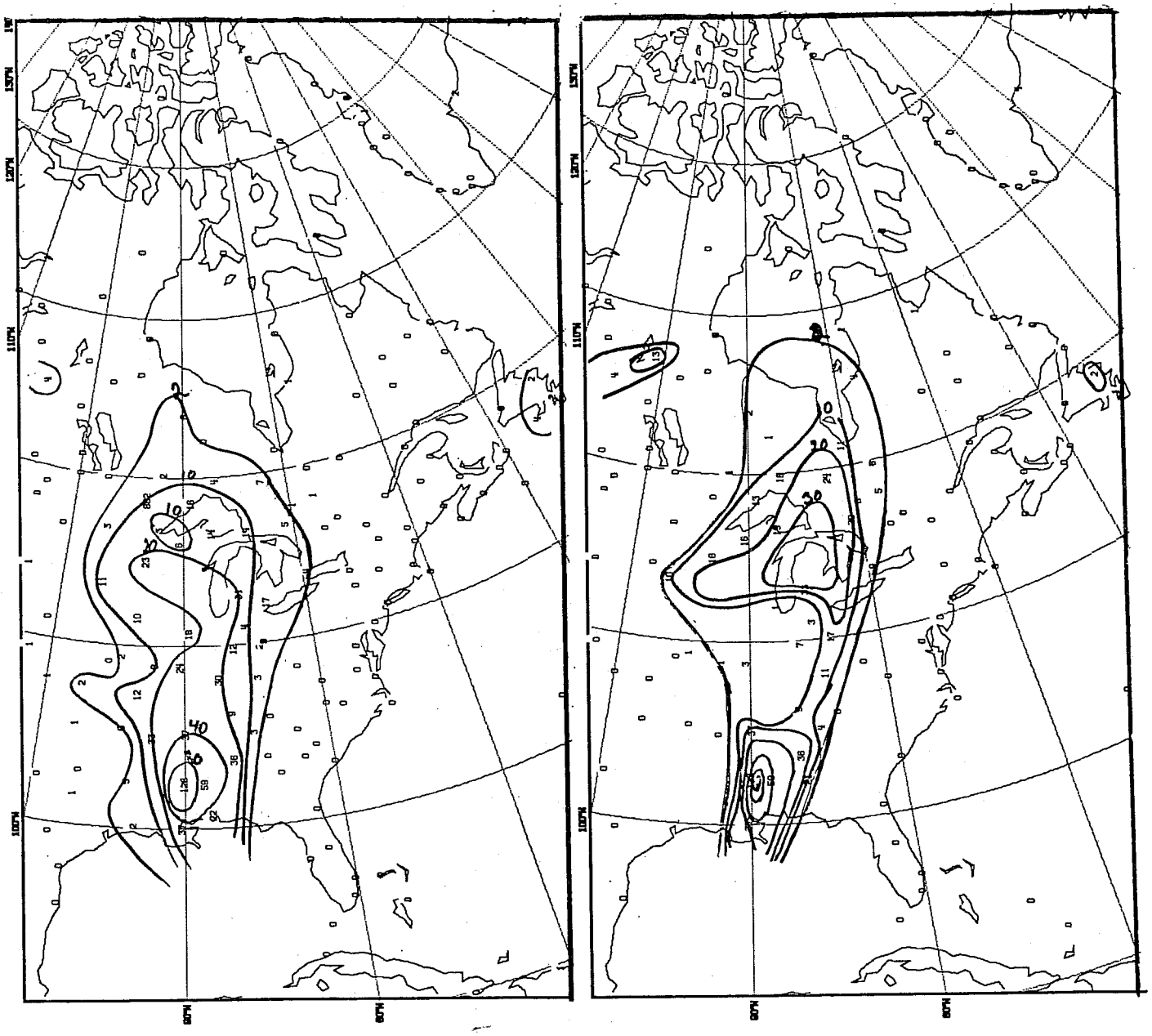

Fig. 46 Observed precipitation accumulated over 24 hours
Left: for the time period 12 GMT 13 April - 12 GMT 14 April 1983 (corresponding to the spectral forecast in Fig. 37).
Right: for the time period 00 GMT - 24 GMT 14 April 1983 (corresponding to the gird-point forecast in Fig. 37). (Unit: mm).

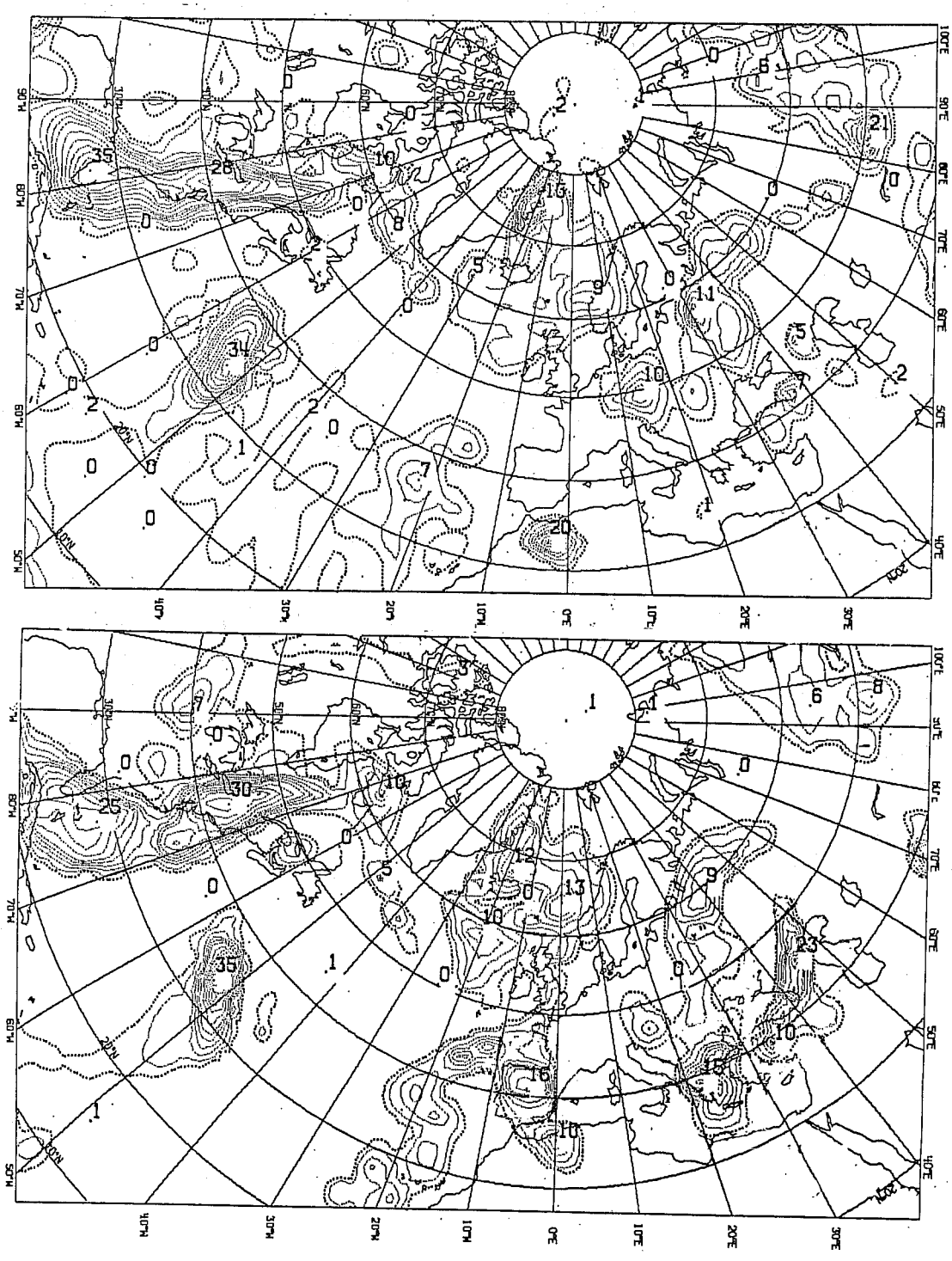

Fig. 47 Forecast precipitation accumulated over 24 hours for the 72 hour spectral forecast from 16 April 1983 (top) and the 84 hour grid-point forecast from 16 April 1983 (bottom). (Unit: mm).

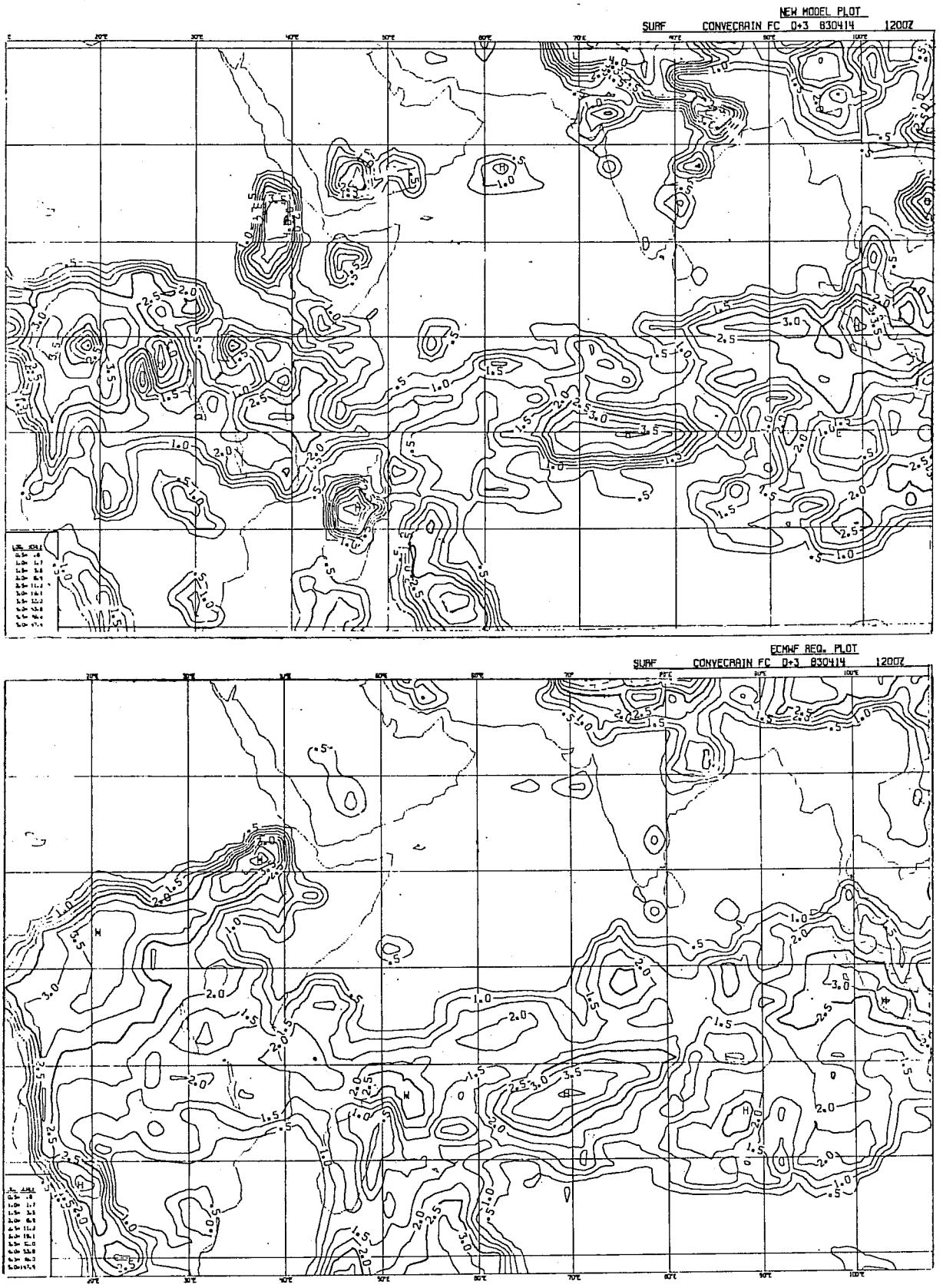

Fig. 48 72 hour accumulated precipiation in the spectral forecast from 14 April 1983 (top) and the grid-point forecast from 14 April 1983 (bottom). (Unit: log; 1=1.7mm, 2=6.4mm, 3=19.1mm, 4=53.6mm, 5=147.4mm)

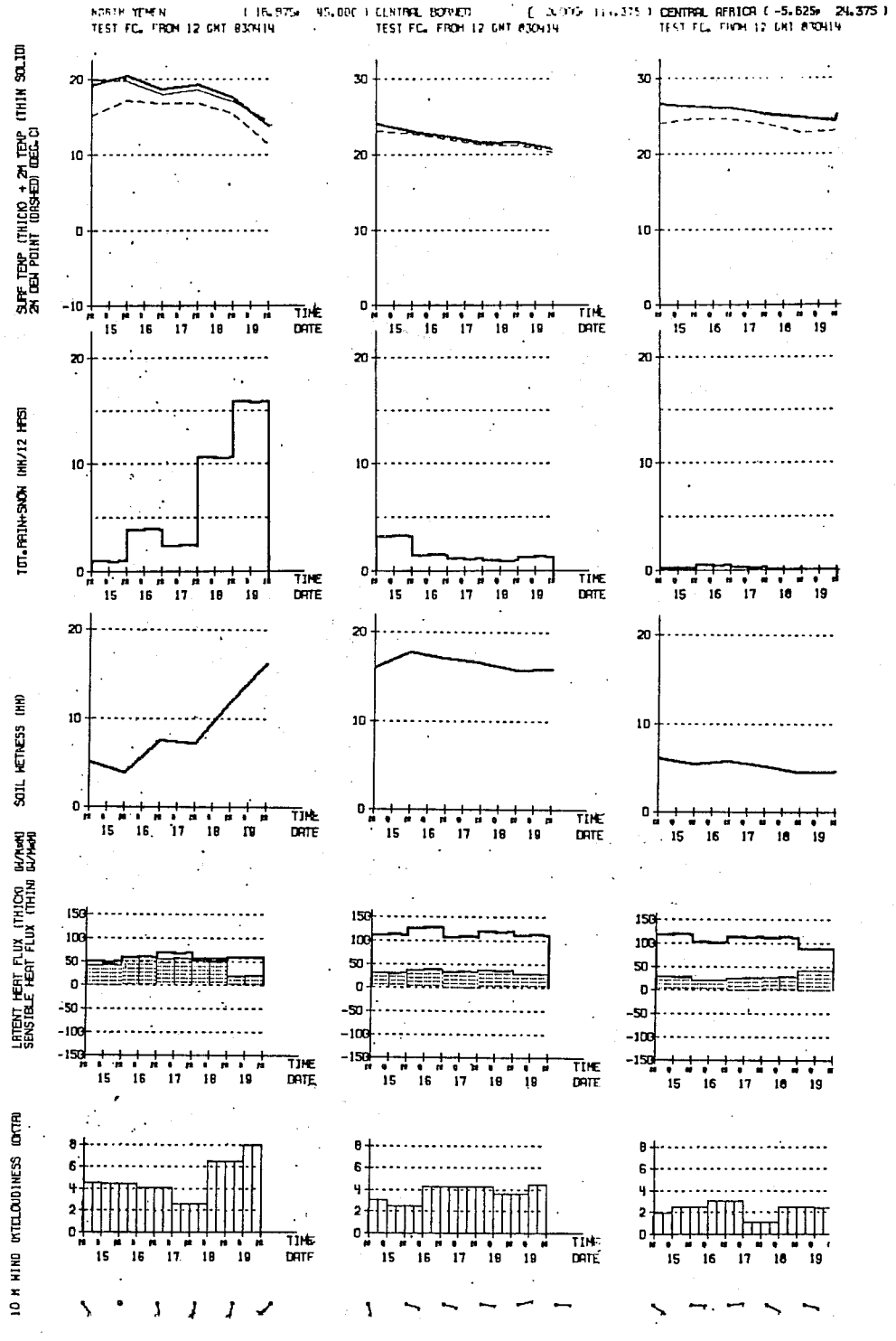

Fig. 49 Surface parameter meteograms for North Yemen (left), Central Borneo (middle) and Central Africa (right) from the spectral forecast of 14 April 1983.

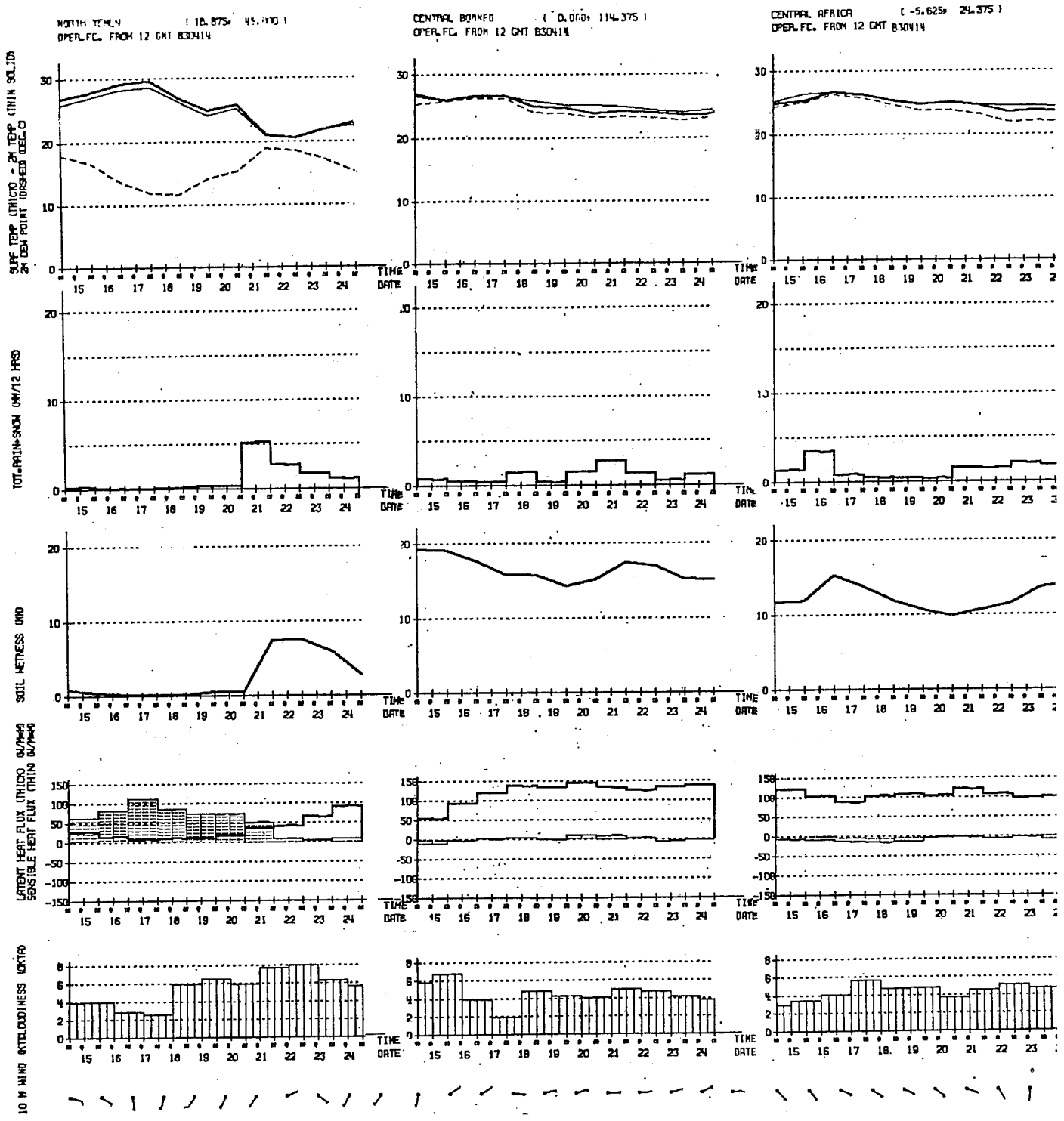

Fig. 50 Surface parameter meteograms for North Yemen (left), Central Borneo (middle) and Central Africa (right) from the grid-point forecast from 14 April 1983.

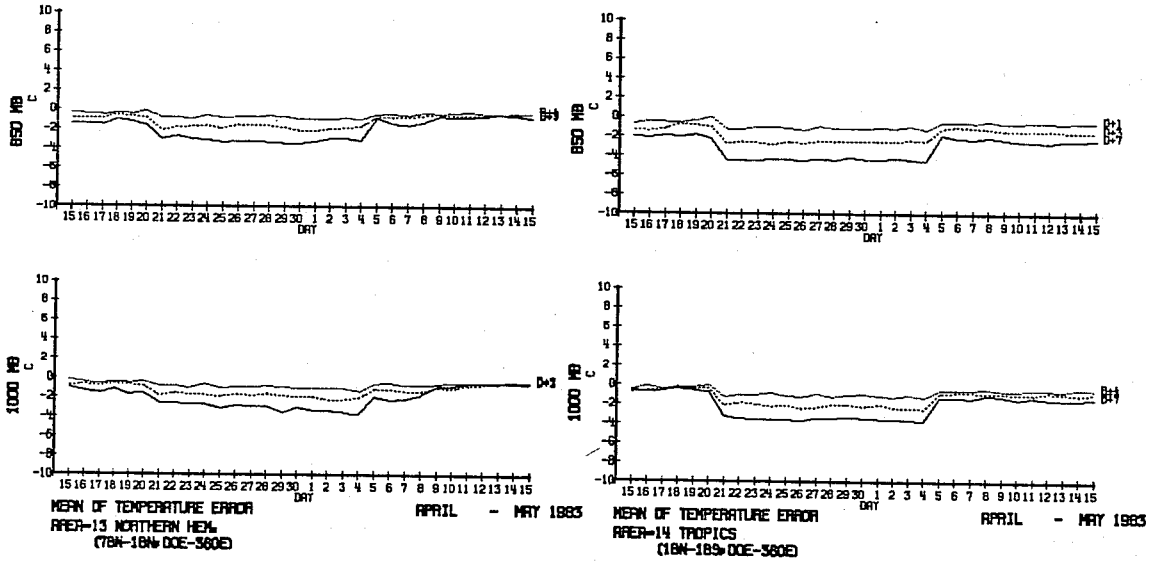

Fig. 51 Mean error of temperature in degrees Celsius for 850 mb (top) and 1000 mb (bottom) over the Northern Hemisphere (left) and the tropic (right), for day 1, day 3 and day 7 of the forecast in the period 15 April to 15 May 1983.